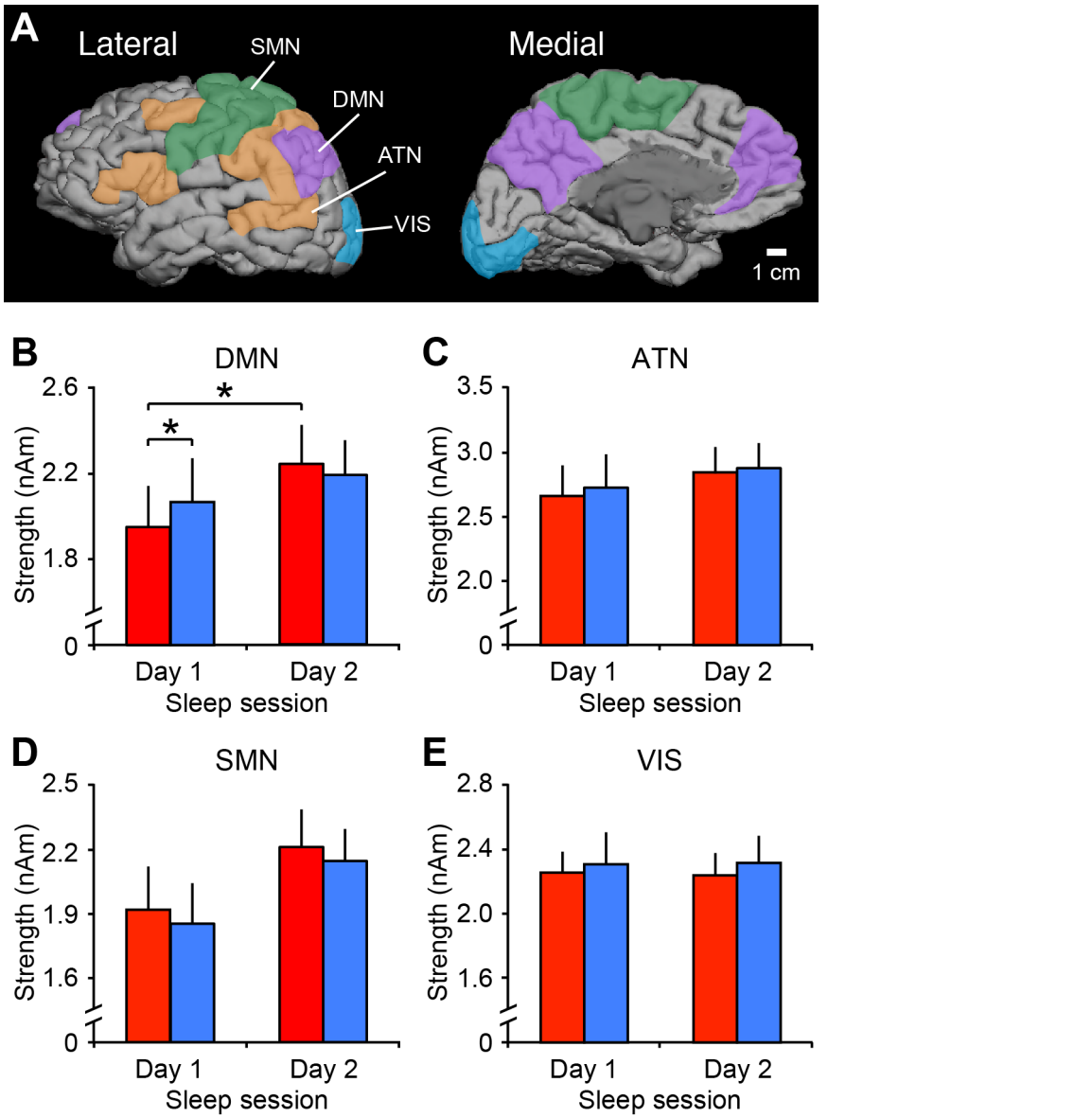

Figure S1: SWA strength in the networks for Experiment 1, related to Figure 1.
(**A**) The brain regions included in each network for calculation of SWA. The left hemisphere of a representative subject is shown in the folded format of the brain [S1, S2] for lateral and medial views. The default-mode network (DMN) is shown in purple, the attention network (ATN) in orange, the sensorimotor network (SMN) in green, and the visual network (VIS) in cyan. Scale bar, 1cm. See **1.7 Brain networks** in **Supplemental Experimental Procedures** for details. (**B-E**) The red bars indicate the SWA strength (N = 11, mean ± SEM) in networks of the left hemisphere, and the blue bars indicate the right hemisphere, on day 1 and day 2. SWA in the DMN (**B**, the same as **Figure 1A**), the ATN (**C**), the SMN (**D**), and the VIS (**E**) during slow-wave sleep. Asterisks indicate the statistical significance described below (*p<0.05, see **#1** for the results of ANOVA). See also (**#2**) regarding the asymmetry index of SWA.

#1: First, we conducted a 4-way repeated measures ANOVA on SWA with factors being network (DMN, ATN, SMN, VIS), hemisphere (left, right), sleep stage (slow-wave sleep, stage 2 sleep), and sleep session (day 1, day 2). Since there was a significant 4-way interaction (see **Table S2**), we proceeded to the next level analyses, that is, a 3-way repeated measures ANOVA with factors being sleep stage, hemisphere, and sleep session for each network (**Table S2**), as a simple effect test, using separate error terms (see **1.8 Statistical analyses**). Since a significant 3-way (sleep stage x hemisphere x sleep session) interaction was significant only for the DMN, we further proceeded to the next level analyses, that is, a 2-way repeated measures ANOVA with factors being hemisphere and sleep session for the DMN for each of slow-wave sleep and stage 2 sleep (**Table S2**) as a simple-simple effect test, but not for other networks. There was a significant 2-way (hemisphere x sleep session) interaction only for slow-wave sleep ($F_{1, 10}$=10.03, p=0.010), not for stage 2 sleep (**Table S2**). These results indicate that the 4-way interaction in the omnibus test originated in the DMN during slow-wave sleep. Finally, since the interaction of the 2-way repeated measures ANOVA was significant only for the DMN during slow-wave sleep, we conducted post-hoc paired *t*-tests on the SWA strength within the DMN during slow-wave sleep to examine in which hemisphere SWA strength was changed between sleep sessions, as a simple-simple-simple effect test. The post-hoc *t*-tests indicated that SWA strength in the *left* DMN was significantly decreased on day 1 compared to day 2 (**Figure S1B**; day 1 vs. day 2 in the left DMN, t_{10}= 2.69, p=0.023, d=0.8). There was no significant difference between days in SWA in the *right* DMN (day 1 vs. day 2 in the right DMN, t_{10}= 0.97, p=0.355, *n.s.*). We also found that SWA in the left hemisphere decreased to a significantly greater degree compared to the right hemisphere on day 1 in the DMN (**Figure S1B**; left vs. right on day 1, t_{10}= 2.59, p=0.027, d=0.8), but that there was no significant difference between hemispheres on day 2 (left vs. right on day 2, t_{10}= 1.65, p=0.129, *n.s.*).

#2: The SWA asymmetry index also supports that asymmetry of SWA is significant only for the DMN for the first sleep session according to the following analyses. We obtained SWA asymmetry indices ([left SWA - right SWA]/[left SWA + right SWA]) for 4 networks. A 2-way repeated measures ANOVA, with the factors of network (DMN, ATN, SMN, VIS) and sleep session (day 1, day 2), was conducted on the SWA asymmetry indices. If the FNE was associated with asymmetric SWA specifically in the DMN among the 4 networks examined, a significant interaction of network and sleep session should be obtained. Indeed, the interaction was statistically significant ($F_{3, 30}$= 5.34, p = 0.005). Neither the main effect of network ($F_{3, 30}$=1.64, p=0.200, *n.s.*) nor sleep session ($F_{1, 10}$= 0.29, p=0.599, *n.s.*) was significant. Given that the 2-way interaction between network and sleep session was significant, we next tested a simple main effect of sleep session for each network. Post-hoc paired *t*-tests showed that none of ATN, SMN, and VIS showed a significant difference between sleep sessions (day 1 vs. day 2; ATN: t_{10}= 0.24, p =0.816, *n.s.*; SMN: t_{10}= 0.32, p=0.756, *n.s.*; VIS: t_{10}= 1.40, p=0.193, *n.s.*). The asymmetry indices were significantly different between sleep sessions only in the DMN (day 1 vs. day 2, t_{10}= 3.16, p=0.010, d=1.0). In addition, the asymmetry index in the DMN was significantly different from 0 on day 1 (day 1 vs. 0 in the DMN, t_{10}= 2.37, p=0.039, d=0.7), whereas it was not on day 2 (day 2 vs. 0 in the DMN, t_{10}= 1.33, p=0.215, *n.s.*). The results indicate that SWA during slow-wave sleep in the DMN was significantly weaker in the left hemisphere compared to the right, and that the impact of the FNE was specific to the DMN only on day 1.

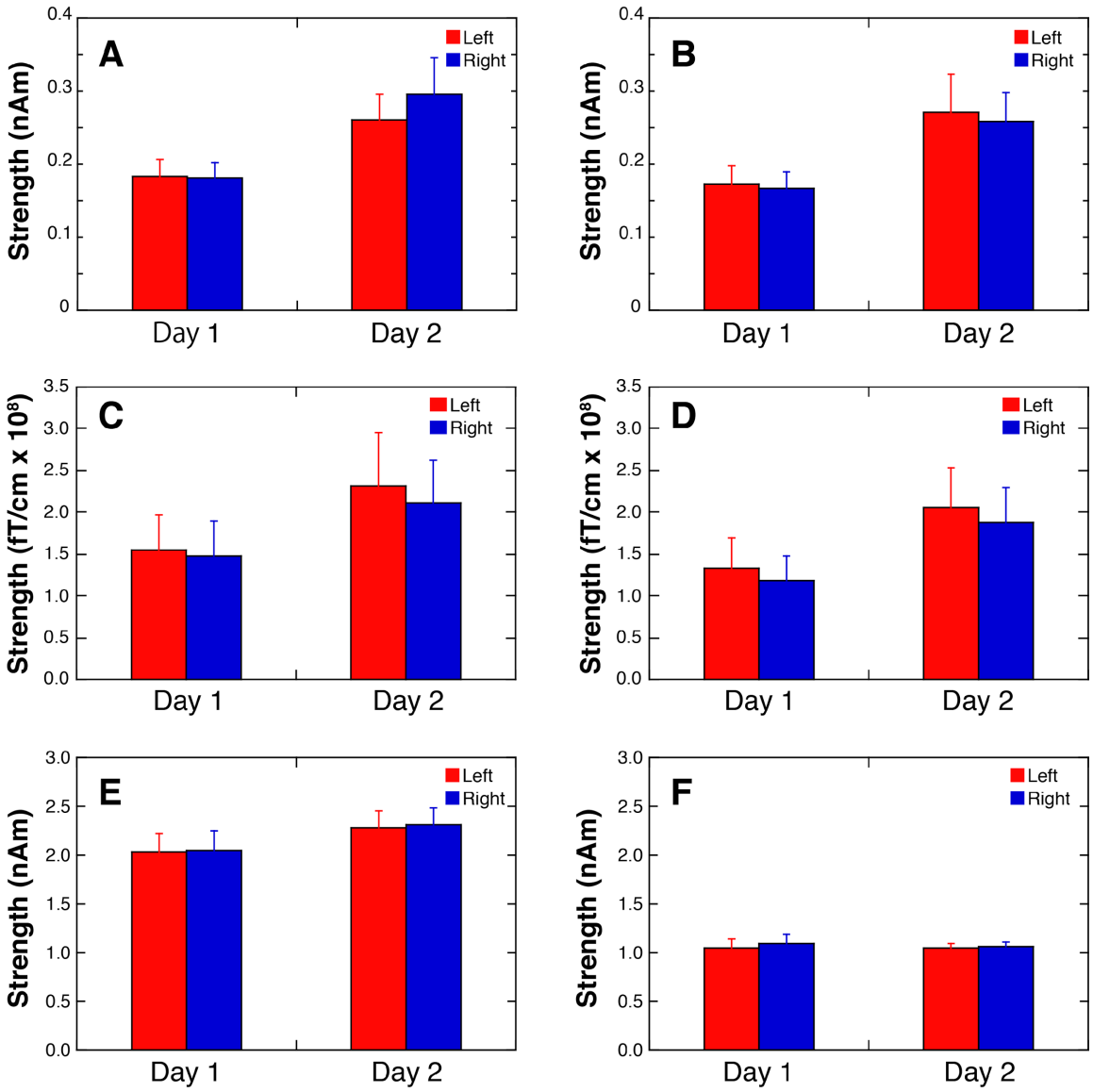

Figure S2: Additional data on SWA for Experiment 1, related to Figure 1.
Red bars show activities in the left hemisphere, and blue bars the right hemisphere. (**A**) 0.5 Hz activity associated with K-complexes during stage 2 sleep for days 1 and 2 for DMN. (**B**) 0.5 Hz activity associated with K-complexes during stage 2 sleep for days 1 and 2 for SMN. No interhemispheric asymmetry in 0.5 Hz activity associated with K-complexes was found (see **#3** for detailed statistical analysis). (**C**) Sensor-space MEG without source-localization for DMN. (**D**) Sensor-space MEG without source-localization for non-DMN. No clear interhemispheric asymmetry in sensor space MEG SWA was observed (see **#4** for detailed statistical results). (**E**) SWA in the re-defined SMN that excludes the hand area during slow-wave sleep. (**F**) SWA in the re-defined SMN that excludes the hand area during stage 2 sleep. There was no interhemispheric asymmetry in SWA in the SMN which does not include the cortical regions that represent the hand area (see **#5** for more details).

#3: We found that the regional interhemispheric asymmetry of SWA in the DMN in association with the FNE was specific to slow-wave sleep, as shown in **Figure S1**. However, one may wonder whether such regional interhemispheric asymmetry can be found in SWA associated with K-complexes during stage 2 sleep. Thus, we tested whether SWA associated with K-complexes shows regional interhemispheric asymmetry in association with the FNE. We investigated 0.5 Hz activity in particular, because 0.5 Hz activity is a main slow component of K-complexes [S3]. The SMN was included in addition to the DMN in the analysis because K-complexes are thought to be strongly associated with sensory areas [S4-S6].

K-complexes were detected in accordance with the AASM criteria [S7]. The detection of a K-complex was based on the C3 channel, and if C3 was too noisy, the C4 channel was used. To obtain 0.5 Hz activity of K-complexes, we analyzed short time epochs that cover ± 3 sec from the negative peak of a K-complex (a total of 6 sec epoch). If a 6-sec epoch contained slow waves or arousals, this epoch was excluded from further analysis so that the computation was focused on K-complexes. A Morlet wavelet analysis was conducted and the MNE model [S8, S9] was used to source-localize the 0.5 Hz activity and the mean 0.5 Hz activity was obtained for the DMN and SMN in both hemispheres. The results of the analysis are as follows.

First, there was no significant difference in the number of K-complexes detected between days (8.5 ± 1.74 for day 1, and 9.5 ± 2.33 for day 2, Wilcoxon singed-rank test, z_{10}=0.53, p=0.593, *n.s.*).

Next, we applied a 3-way repeated measures ANOVA with factors being network (DMN vs. SMN), hemisphere (left vs. right), sleep session (day 1 vs. day 2) on the 0.5 Hz activity. If the 0.5 Hz activity shows hemispheric asymmetry in association with the FNE, similarly to SWA, we should expect to see a 2-way interaction of hemisphere x sleep session, or a 3-way interaction of network x hemisphere x sleep session, if the 0.5 Hz activity of DMN and SMN are differently involved in the FNE. However, the results did not show any of significant 3-way ($F_{1,8}$=2.72, p=0.138) and 2-way (network x hemisphere: $F_{1,8}$=0.59, p=0.463; network x sleep session: $F_{1,8}$=0.26, p=0.627; hemisphere x sleep session: $F_{1,8}$=0.00, p=0.980) interactions. Moreover, none of the factors showed a significant main effect (network: $F_{1,8}$=0.25, p=0.633; hemisphere: $F_{1,8}$=0.03, p=0.860; sleep session: $F_{1,8}$=3.00, p=0.122).

The results of these analyses do not support the possibility that SWA associated with K-complexes should show hemispheric asymmetry during stage 2 sleep in association with the FNE. Along with the information shown in (**#1**) above, these results suggest that the regional hemispheric asymmetry of SWA is specific to slow-wave sleep.

Then, the question may arise as to why K-complexes did not show any difference in association with the FNE, given that a function of K-complexes may be to protect sleep through inhibition of sensory areas during sleep [S4, S10]. While this may be beyond the scope of the present study, it is possible that the inhibition of cross-modal sensory areas involved in K-complexes is an intrinsic property of sleep itself, not subject to modulation by the FNE.

#4: We tested whether regional hemispheric asymmetry of SWA can be seen in the sensor-space MEG data without any source-localization technique. We conducted spectral analyses for MEG during slow-wave sleep.

A fast-Fourier transformation was applied to the MEG data in 5-second epochs and smoothed with a tapered cosine window to obtain spectral data for SWA (1–4 Hz). Six epochs were averaged to yield spectral data of 30 s. The spectral data obtained during slow-wave sleep was averaged for each region in the following way. The powers of SWA were measured from anterior sensors, which are near the medial frontal [S11] as well as parietal sensors near parietal cortices [S12]. The powers were averaged to represent SWA strength for the DMN. Likewise, the powers of SWA from central sensors near the sensory-motor [S13] and occipital sensors near the visual cortex [S14] were averaged to represent SWA strength for the control regions (non-DMN). Eight gradiometer sensors were selected for each region and hemisphere (32 sensors in total; left DMN: 0612, 0613, 0642, 0643, 1632, 1633, 1642, 1643; right DMN: 1022, 1023, 1032, 1033, 2442, 2443, 2432, 2433; left non-DMN 0442, 0443, 1812, 1813, 1932, 1933, 2142, 2143; right non-DMN: 1132, 1133, 2222, 2223, 2332, 2333, 2132, 2133; each number corresponds to the sensor-location identification number, Elekta Neuromag Oy, Helsinki, Finland). We used only data from the gradiometers for subsequent analyses and excluded magnetometers. Gradiometers and magnetometers use

different coils and we needed to avoid mixing them. Gradiometers are also placed more densely compared to magnetometers.

The source-localized data clearly indicated that the regional hemispheric asymmetry in SWA was present only in the DMN, and only on day 1 during slow-wave sleep (**Figure 1A**). If this pattern were evident in the sensor-space data, a significant 3-way interaction should have been observed when a 3-way repeated measures ANOVA was performed on measures of SWA during slow-wave sleep (factors = region (DMN vs. non-DMN), hemisphere (left vs. right), and sleep session (day 1 vs. day 2)). However, no significant 3-way interaction was found ($F_{1, 10}$= 0.38, p=0.552, *n.s.*). There was a significant main effect for sleep session ($F_{1, 10}$= 8.64, p=0.015). No other main effects or interactions were significant (region, $F_{1, 10}$= 4.66, p=0.056, *n.s.*; hemisphere, $F_{1, 10}$= 1.38, p=0.267, *n.s.*; region x hemisphere, $F_{1, 10}$=0.02, p=0.879, *n.s.*; region x sleep session, $F_{1, 10}$=0.01, p=0.917, *n.s.*; hemisphere x sleep session, $F_{1, 10}$= 0.68, p=0.428, *n.s.*). These results suggest that the sensor-space MEG data are not sufficiently sensitive to the detection of hemispheric asymmetry in spontaneous SWA in the DMN at least with regard to the FNE.

#5: Regional hemispheric asymmetry of SWA in the DMN on day 1 cannot be explained by the handedness in the present study for the following three reasons.

First, the present study has found a unique hemispheric asymmetry in SWA located in the DMN only for the first sleep session, but not for the second sleep session. The handedness for a subject was consistent across these two sleep sessions. Thus, it is difficult to attribute the handedness to hemispheric asymmetry of SWA in the DMN during the first sleep session.

Second, the hemispheric asymmetry found in the first sleep session was specific to the DMN among the 4 networks examined. Since the DMN does not include cortical regions that represent the hands (the hand area), it is difficult for the handedness to account for the reduced SWA in the DMN found during the first sleep session.

Third, we have confirmed that the SMN excluding the hand area does not show hemispheric asymmetry of SWA during the first sleep session. We conducted the following analysis to test whether the SMN without the hand area is impacted by the handedness, since the original SMN included the cortical hand area. We re-defined the SMN so that the SMN excludes the hand area. The hand area was defined by a typical fMRI paradigm of finger tapping (for instance [S15]), morphed into a common anatomical space, and projected back to localize the hand area in the individual cortical space [S1]. We applied a 3-way repeated measures ANOVA with factors being sleep stage (stage 2 sleep vs. slow-wave sleep), hemisphere (left vs. right), and sleep session (day 1 vs. day 2) on SWA in the SMN without the hand area. The results did not support hemispheric asymmetry of SWA in the SMN in the first sleep session (and in the second) since there was no significant 3-way interaction ($F_{1,10}$=0.24, p=0.637). Thus, the SMN does not show any hemispheric asymmetry of SWA in the SMN, irrespective of whether the hand area was included or not.

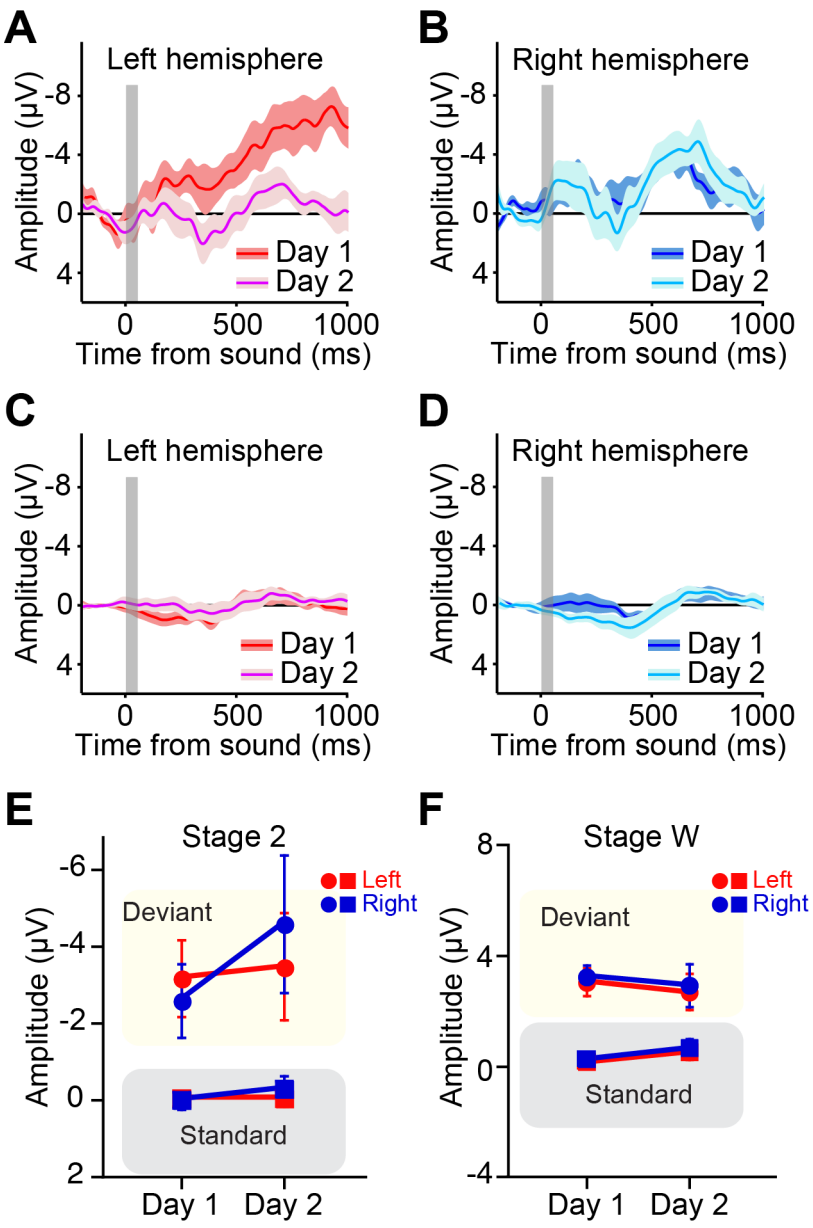

Figure S3: Additional data on evoked responses for Experiment 2, related to Figure 2.
(**A, B**) The grand-averaged brain responses to *deviant* sounds time-locked to the sound onset in the left (**A**) and right (**B**) hemispheres during slow-wave sleep. See additional comment (**#6**) below regarding a possible relation between the brain responses and K-complexes. (**C, D**) The grand-averaged brain responses to *standard* sounds time-locked to the sound onset in the left (**C**) and right (**D**) hemispheres. See additional information (**#7**) regarding interhemispheric asymmetry of the brain responses with the FNE during slow-wave sleep, based on the 3-way repeated measures ANOVA results. (**E**) The mean amplitudes of the brain responses to *deviant* and *standard* sounds in the left (red) and right (blue) hemispheres (μV) during stage 2 sleep. See additional information (**#8**) regarding no interhemispheric asymmetry of the brain responses during stage 2 sleep, based on ANOVA results. (**F**) The mean amplitudes of the brain responses to *deviant*

and *standard* sounds in the left (red) and right (blue) hemispheres (μV) during stage W. See additional information (**#9**) regarding no interhemispheric asymmetry of the brain responses during stage W associated with the FNE. Note that in these evoked responses analyses, the brain activity during pre-stimulus interval did not contribute to the observed results. We have confirmed this by calculating the nadir-to-peak amplitude of evoked responses [S16, S17], which essentially showed the same results with the subtraction method used for the evoked response analyses. See additional comment (**#10**) regarding the robust interhemispheric asymmetry of evoked potentials.

#6: It is noticeable that that the evoked brain responses by deviant sounds associated with the FNE shown in **Figure S3A** may be a component of evoked K-complexes [S17, S18]. It is possible that the increased amplitude of the N3 component in the left hemisphere in the present study shares same underlying mechanisms for evoked K-complexes. Functions of evoked K-complexes have been controversial and are still under debate [S4, S10, S19] regarding whether these functions produce awakening or conversely protect sleep against incoming sensory information. In any case, it might be important to remove impacts of the FNE when functions of evoked K-complexes are investigated in the future.

#7: We tested whether the amplitude of brain responses showed interhemisperic asymmetry only on day 1 to deviant sounds during slow-wave sleep. We conducted a 3-way repeated measures ANOVA with factors of sound type, hemisphere, and sleep session during slow-wave sleep on the mean amplitude of brain responses. If hemispheric asymmetry in the mean amplitude of brain responses during slow-wave sleep to deviant sounds is evident only on day 1, we should see a significant 3-way interaction in the ANOVA. The results indeed showed the significant interaction ($F_{1, 12}$=9.20, p=0.010). Based on this significant 3-way interaction, we then conducted a 2-way repeated measures ANOVA with factors of hemisphere and sleep session on the mean amplitude of brain responses for each sound type as subsequent post-hoc interaction analyses. The results of 2-way repeated measures ANOVA for the deviant sounds showed a significant interaction between hemisphere and sleep session ($F_{1, 12}$=10.20, p=0.008). The main effects for sleep session or hemisphere were not significant (hemisphere, $F_{1, 12}$=1.46, p=0.250, *n.s.*; sleep session, $F_{1, 12}$=3.80, p=0.075, *n.s.*). On the other hand, in a 2-way repeated measures ANOVA for the standard sounds neither factors nor their interaction was significant (hemisphere, $F_{1, 12}$=3.39, p=0.090, *n.s.*; sleep session, $F_{1, 12}$=0.09, p=0.774, *n.s.*; hemisphere x sleep session, $F_{1, 12}$=0.21, p=0.654, *n.s.*). See the main text (**Figure 2A**) regarding the results of post-hoc *t*-tests as a simple-simple effect test for the brain responses for the deviant sounds. These results suggest that the asymmetry in brain responses associated with the first sleep session occurred only to deviant sounds during slow-wave sleep.

#8: A 3-way repeated measures ANOVA was conducted to test whether brain responses during stage 2 sleep were affected by any of the factors such as sound type (deviant, standard), hemisphere (left, right), and sleep session (day1, day 2). If there was hemispheric asymmetry in brain responses to sounds during stage 2 sleep, a significant 3-way interaction should be observed. However, the results showed that the 3-way interaction was not significant ($F_{1, 12}$=1.16, p=0.307, *n.s.*). Sound type was the only significant main effect ($F_{1, 12}$=10.03, p=0.010). Neither main effect of hemisphere ($F_{1, 12}$= 0.28, p = 0.608, *n.s.*) nor sleep session ($F_{1, 12}$=1.14, p=0.310, *n.s.*) was significant. In addition, there were no significant 2-way interactions (sound type x hemisphere, $F_{1, 12}$=0.05, p=0.836, *n.s.*; sound type x sleep session, $F_{1, 12}$=0.80, p=0.391, *n.s.*; hemisphere x sleep session, $F_{1, 12}$=2.74, p=0.129, *n.s.*). These results suggest that the hemispheric asymmetry in brain response to deviant sounds associated with the FNE did not occur during stage 2 sleep.

#9: Is it possible that the interhemispheric asymmetry of the brain responses associated with the FNE appears during wakefulness? To test this possibility, we conducted a similar oddball paradigm experiment to that shown in previous studies [S20-S22] immediately before sleep sessions and collected brain response data during the wakefulness session. The same group of subjects as in Experiment 2 participated in this experiment. The wakefulness session lasted for 10 min. Subjects sat on a bed in a sleep chamber, and sounds were presented to subjects' ears through earphones. Subjects were instructed to read a book provided by the experimenter and to ignore the presented sounds [S20]. This instruction was provided according to previous studies [S20, S21], because subjects were also instructed to ignore the sounds if they

heard them during the sleep session (**2.2 Experimental design** in **Supplemental Experimental Procedures**). Subjects were instructed to refrain from making large movements and not to sleep during the wakefulness session. In regard to brain responses during wakefulness, we analyzed the P3 [S23] component from EEG data acquired during the wakefulness session. We did not analyze the N3 component, because the N3 is known to be a sleep-specific component, and indeed, we did not detect N3 at all during wakefulness. P3 is also one of the most frequently examined evoked brain potentials during wakefulness and has been shown to indicate brain responsiveness to external stimuli (the oddball paradigm, specifically) while subjects are awake [S23]. Note that since P3 amplitude decreases markedly as sleep progresses [S24], we did not examine P3 during sleep sessions (**2.4 Analysis of brain responses to auditory stimuli** in **Supplemental Experimental Procedures**). To have the same experimental procedure as the previous research, the sound intensity was set to 45dB, which is an optimal sound intensity for P3 component suggested by previous studies [S22]. Other aspects of the oddball paradigm were identical to those used in the sleep session (**2.3 Auditory stimuli** in **Supplemental Experimental Procedures**).

To obtain the P3 component, 3 centro-parietal channels for each hemisphere (left: CP1, CP3, CP5; right, CP2, CP4, CP6) were analyzed. The centro-parietal area was chosen because P3 has been reported to be dominant in this area [S23, S25]. All the data were first inspected automatically then visually, and any trials (1 trial = 1000 ms) that were either contaminated by large motion artifacts or showed more than 100 μV in any of the channels listed above were excluded from further analyses. The amplitudes of EEG measured during the 200 ms pre-stimulus period (from -200 to 0 ms) were averaged. The mean value of the pre-stimulus period was subtracted from the 1000 ms post-stimulus period to normalize the amplitude for each trial. Trials were averaged for each sound type (deviant, standard), hemisphere (left, right), and sleep session (day 1, day 2), for each subject to obtain averaged brain responses. Then, the amplitude of the positive peak in the averaged brain responses occurring between the 200 – 400 ms post-stimulus time window was used to obtain the peak of P3 [S23].

We conducted a 3-way repeated measures ANOVA to test whether brain responses during wakefulness (**Figure S3F**) were affected by factors including the sound type (deviant, standard), hemisphere (left, right), and sleep session (day1, day 2). If there was hemispheric asymmetry in brain responses to sounds even during wakefulness, there should be a significant 3-way interaction. However, the results showed that the 3-way interaction was not significant ($F_{1, 12}$=0.00, p=0.978, *n.s.*). The only significant main effect was sound type ($F_{1, 12}$=30.72, p<0.001). Neither main effect of hemisphere ($F_{1, 12}$=1.38, p=0.264, *n.s.*) nor sleep session ($F_{1, 12}$=0.01, p=0.923, *n.s.*) was significant. In addition, there were no significant 2-way interactions (sound type x hemisphere, $F_{1, 12}$=0.04, p=0.843, *n.s.*; sound type x sleep session, $F_{1, 12}$=1.81, p=0.203, *n.s.*; hemisphere x sleep session, $F_{1, 12}$=0.01, p=0.907, *n.s.*).

These results rule out the possibility that the interhemispheric asymmetry of the brain responses associated with the FNE appears during wakefulness.

Furthermore, these results rule out the possibility that the reduced N3 response to deviant sounds during slow-wave sleep on day 2 is due to a general effect of habituation. Since the P3 component is thought to reflect automatic orientation of attention [S23, S26, S27], the P3 component during wakefulness should have been reduced on day 2 if habituation to deviant sounds occurred. However, the P3 component on day 2 was not significantly reduced compared to day 1.

#10: Although regional asymmetric SWA in the DMN required source-localization techniques, the asymmetry in the evoked brain response was apparent without source-localization. This distinction may be explained by a possible larger amplitude of evoked brain activities than spontaneous activities [S22, S28]. Evoked brain responses might be a useful marker for elucidating hemispheric asymmetry of sleep without source-localization techniques.

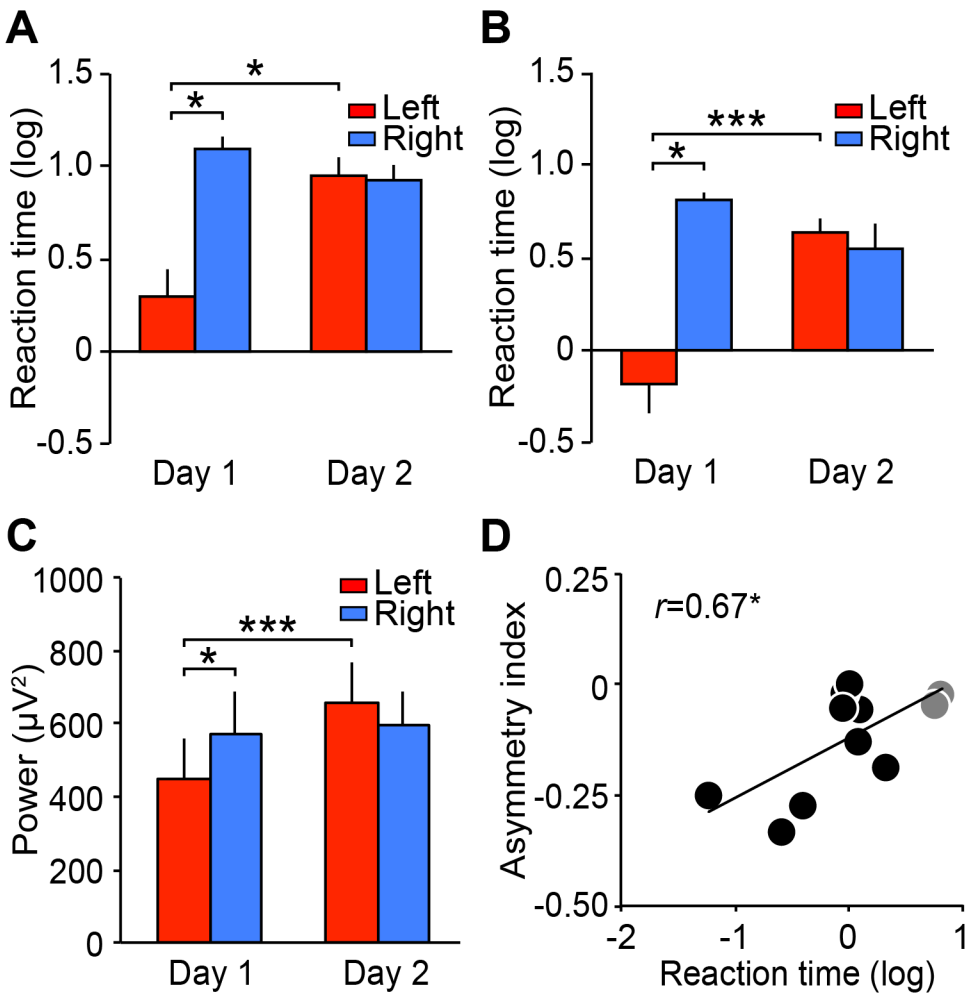

Figure S4: Additional data on behavioral responses for Experiment 3, related to Figure 4.
(**A**) Reaction time between a deviant sound and tapping for the left-hemisphere trial (red bars) and the right-hemisphere trial (blue bars) on day 1 and day 2. The Mann-Whitney U test indicated that the reaction time for the left-hemisphere trials was significantly faster than the right-hemisphere trials on day 1 (p=0.036), and the reaction time for the left-hemisphere trials on day 1 was also significantly faster than on day 2 (p=0.011). *p<0.05. (**B**) Reaction time from a deviant sound to awakening for the left-hemisphere trials (red bars) and the right-hemisphere trials (blue bars) on day 1 and day 2. The Mann-Whitney U test indicated that the reaction time for the left-hemisphere trials was significantly faster than the right-hemisphere trials on day 1 (p=0.036), and the left-hemisphere trials on day 1 was significantly faster than the left-hemisphere trials on day 2 (p=0.003). The values are mean ± SEM. ***p<0.005, *p<0.05. See additional comment below (**#11**) regarding hemispheric asymmetry in the reaction time, which was largely driven by time before awakening occurred. (**C**) The regional SWA measured by a spectral analysis on EEG for the left (red bars) and right (blue bars) hemispheres (see **3.7 Spectral power and correlation analyses** in **Supplemental Experimental Procedures**). The values are mean ± SEM. ***p<0.005, *p<0.05. See additional information (**#12**) below regarding the statistical results on SWA. (**D**) Scatter plots for the asymmetry index of SWA (see **3.7 Spectral power and correlation analyses** in **Supplemental Experimental Procedures**) against the time interval from the deviant sound to awakening (log) on day 1. The black plots are for the subjects who woke up from the left-hemisphere trials, and the gray plots are for

the subjects who woke up from the right-hemisphere trials. A significant positive correlation between the SWA asymmetry index and the time interval was found on day 1 (r=0.67, p=0.025), but not on day 2 (r=-0.01, p=0.986, *n.s.*). A significant correlation was also obtained between the SWA asymmetry index and the time between the deviant sound and tapping on day 1 (r=0.71, p=0.014) but not on day 2 (r=0.11, p=0.749, *n.s.*). *p<0.05. See additional information (**#13**) below regarding the asymmetry index of SWA. Also see comment below (**#14**) regarding the robust interhemispheric regional SWA without source-localization.

#11: It is worth noting that the shorter reaction time from a deviant sound to tapping in the left-hemisphere trials on day 1 (**Figure S4A**) was mainly driven by the time interval from the deviant sound to awakening while subjects were asleep (**Figure S4B**), and not by the time interval from the awakening to tapping after subjects were woken, as described below.

The reaction time from a deviant sound to tapping, shown in **Figure 4B**, can be divided into 2 temporal phases; the first is the elapsed time from a deviant sound to awakening (**Figure S4B**), and the second is the elapsed time from awakening to tapping. We analyzed these 2 phases separately, and tested which of these phases (or both) accounted for the hemispheric asymmetry in the reaction time on day 1.

First, the elapsed time for the first temporal phase was compared between the left-hemisphere trials and the right-hemisphere trials on day 1 and day 2. The amount of time to awakening in the left-hemisphere trials was significantly smaller than in the right-hemisphere trials on day 1 (Mann-Whitney U test, p=0.036; **Figure S4B**). The amount of time to awakening for the left-hemisphere trials was significantly smaller on day 1 than day 2 (Mann-Whitney U test, p=0.003). Next, the second temporal phase (from awakening to tapping) was not significantly different either between hemispheres on day 1 (Mann-Whitney U test, p=0.073) or between days for the left-hemisphere trials (Mann-Whitney U test, p= 0.050).

These results suggest that the faster behavioral outcomes on day 1 shown in **Figure 4B** were mostly due to a faster response in the sleeping brain (in the left hemisphere) to wake itself up quickly when it needs to carry out a task, and not due to a faster response after the brain was woken.

#12: The regional SWA showed hemispheric asymmetry only on day 1. To test whether the regional SWA during slow-wave sleep showed hemispheric asymmetry with the FNE, we conducted a 2-way repeated measures ANOVA, with the factors of hemisphere (left vs. right) and sleep session (day 1 vs. day 2) on SWA. There was a significant hemisphere x sleep session interaction ($F_{1, 10}$=15.35, p=0.003). A main effect of sleep session was also significant ($F_{1, 10}$=5.98, p=0.035). A main effect of hemisphere was not significant ($F_{1, 10}$=0.86, p=0.374, *n.s.*). Given that the 2-way interaction was significant, we next conducted post-hoc *t*-tests to test whether the regional SWA was significantly different between sleep sessions for each hemisphere. The *t*-tests indicated that the left hemisphere showed a significant difference between sleep sessions (the regional SWA was significantly smaller on day 1 than day 2; t_{10}=3.78, p=0.004), but the right hemisphere did not (t_{10}=0.47, p=0.651, *n.s.*). We also found that the regional SWA in the left hemisphere was significantly smaller than the right on day 1 (t_{10}=2.72, p=0.022), but not on day 2 (t_{10}=1.76, p=0.109, *n.s.*).

#13: We tested whether there was a significant difference in the SWA asymmetry index between sleep sessions. A two-tailed *t*-test indicated there was a significant difference between sleep sessions in the SWA asymmetry index (t_{10}=4.84, p<0.001). The SWA asymmetry index on day 1 was significantly different from 0 (*t*-test, t_{10}=3.49, p=0.006), but not on day 2 (*t*-test, t_{10}=1.92, p=0.084, *n.s.*).

#14: These results (**#12** and **#13**) indicate that the interhemispheric asymmetry of SWA measured from scalp EEG near the DMN could be observed on day 1 without source-localization techniques in Experiment 3. One may wonder whether these results are inconsistent with the results in Experiment 1 in which the interhemispheric asymmetry of SWA, measured from sensor-space MEG, was not observable on day 1 without source-localization techniques (**Figure S2C, D**). However, the results from Experiments 1 and 3 do not necessarily contradict to each other. The experimental manipulations were very different between the experiments, and the differences in manipulations might have impacted interhemispheric asymmetry of SWA to a different degree. In Experiment 1, SWA was measured from spontaneous brain activities during

sleep with no auditory stimulation presented or with no behavioral responses requested. In contrast, in Experiment 3, the subjects were presented auditory sounds during sleep, and behavioral responses to sounds were required. We speculate that these manipulations (auditory stimuli and behavioral response) for Experiment 3 might have further increased the need for vigilance, which resulted in a more robust regional interhemispheric asymmetry of SWA than Experiment 1.

Table S1: Sleep parameters for Experiments 1–3, related to Figures 1-4

	Experiment 1		Experiment 2		Experiment 3	
	Day 1	Day 2	Day 1	Day 2	Day 1	Day 2
Sleep-onset latency (min)[a]	21.0 ± 3.88	9.1 ± 2.00	13.0 ± 2.32	6.0 ± 0.72	13.3 ± 2.47	7.2 ± 1.99
WASO (min)[a]	9.0 ± 3.35	1.0 ± 0.44	11.5 ± 2.65	2.6 ± 1.04	14.8 ± 3.42	7.9 ± 2.26
Slow-wave sleep (%)[a,b]	31.6 ± 6.30	48.6 ± 4.23	15.7 ± 2.60	30.3 ± 2.92	13.5 ± 2.86	21.6 ± 4.18
Stage W (%)	21.5 ± 5.21	7.2 ± 1.72	23.4 ± 2.53	8.0 ± 1.32	28.2 ± 4.46	16.3 ± 4.22
Stage 1 sleep (%)	15.4 ± 4.27	10.0 ± 2.39	16.3 ± 2.26	12.4 ± 2.03	20.9 ± 1.69	18.7 ± 2.46
Stage 2 sleep (%)	31.5 ± 3.60	34.3 ± 3.87	44.6 ± 2.86	49.2 ± 3.21	37.3 ± 3.60	43.4 ± 4.26
SE (%)	78.5 ± 5.21	92.8 ± 1.72	76.6 ± 2.53	92.0 ± 1.32	71.8 ± 4.46	83.7 ± 4.22
Total sleep time (min)	78.6 ± 9.48	82.6 ± 7.72	62.8 ± 2.33	65.6 ± 3.50	53.0 ± 2.51	55.4 ± 3.47
Time in bed (min)	119.4 ± 12.8	119.7 ± 13.2	89.2 ± 1.48	91.0 ± 0.63	88.6 ± 1.28	84.0 ± 2.49

WASO, wake after sleep onset. **SE**, sleep efficiency. **Slow-wave sleep%** refers to the percentage of slow-wave sleep occurrence. The total sleep time was defined as the sum of stage 1, 2, and SWS durations within the first sleep cycle. The total recording time indicates the duration of each sleep session (the time interval between lights-off and lights-on). See **4. Comparison of sleep parameters among Experiments 1-3** in **Supplemental Experimental Procedures** for more details about measurement of sleep parameters and statistics.

Values are mean ± SEM.
[a] Significantly different between sleep sessions (day 1 vs. day 2).
[b] Significantly different between Exps.1 vs. 2 as well as between Exps.1 vs. 3.

We confirmed that the FNE occurred in the present study in all the experiments (Exp.1–3) from the sleep-onset latency, WASO, and slow-wave sleep%. The detailed results of the sleep parameters are as follows.

First, we found that the sleep-onset latency, the critical measure for the FNE [S29-S31], was significantly longer on day 1 compared to day 2 in all the experiments. A 2-way mixed design ANOVA (factors=experiment (Exp. 1, 2, and 3), sleep session (day 1 vs. day 2)) was conducted on the sleep-onset latency. There was a significant main effect for sleep session ($F_{1, 32}$=31.90, p<0.001). Neither a main effect for experiment ($F_{2, 32}$=2.32, p=0.114, *n.s.*) nor interaction ($F_{2, 32}$=1.44, p=0.252, *n.s.*) was significant. A post-hoc *t*-test indicated the sleep-onset latency was significantly longer on day 1 than on day 2 (experiment factor was pooled; t_{34} = 5.55, p<0.001, d=0.8). These results indicate that comparable degrees of the FNE occurred in all the experiments.

Second, we found that sleep was more fragmented on day 1 compared to day 2, which further confirmed that the FNE occurred in all experiments. We examined WASO, a measure of sleep fragmentation [S29, S32]. A 2-way mixed design ANOVA (factors=experiment, sleep session) was conducted on WASO. There was a significant main effect for sleep session ($F_{1, 32}$=24.06, p<0.001). Neither a main effect for experiment ($F_{2, 32}$=2.58, p=0.092, *n.s.*) nor interaction ($F_{2, 32}$=0.12, p=0.890, *n.s.*) was significant. A post-hoc *t*-test indicated WASO was significantly larger on day 1 than on day 2 (experiment factor was pooled; t_{34}=5.09, p<0.001, d=1.0). This indicates that sleep was more fragmented on day 1 compared to day 2 in all the experiments to a similar degree, as found in the sleep-onset latency.

Third, we tested whether slow-wave sleep% was smaller on day 1 than on day 2, since it has been suggested that the FNE decreases deep sleep [S29, S33, S34]. The results confirmed this. We conducted a 2-way mixed design ANOVA (factors=experiment and sleep session) on slow-wave sleep%. A main effect for sleep session was significant ($F_{1, 32}$=26.09, p<0.001). A post-hoc *t*-test indicated that the amount of slow-wave sleep% was significantly smaller on day 1 than day 2 (experiment factor was pooled; t_{34}=5.15, p<0.001, d=0.9). This

demonstrates that the amount of the deep sleep was smaller on day 1 than on day 2.

Taken together, sleep was more difficult to be initiated (loner sleep-onset latency), more fragmented (more WASO), and also lighter (smaller slow-wave sleep%) on day 1 compared to day 2 consistently in all the experiments. From these results we concluded that the FNE occurred in all the experiments to comparable degrees, irrespective of differences in experimental designs.

Additionally, we examined which experiments showed a significant difference in slow-wave sleep%, as there was a significant main effect of experiment ($F_{2, 32}$=12.55, p<0.001) on slow-wave sleep%, while an interaction between the two main factors was not significant ($F_{2, 32}$ =1.03, p=0.369, *n.s.*). Post-hoc *t*-tests indicated slow-wave sleep% was significantly larger in Exp. 1 than Exp. 2 (The Scheffé's method, p=0.003) and Exp. 3 (The Scheffé's method, p<0.001). These differences in slow-wave sleep% may be due to the differences in experimental design, since Exp.1 was conducted at night, whereas Exp. 2 and 3 were conducted during daytime.

However, it is worth noting that the degrees of slow-wave sleep% decrease on day 1 were similar in these experiments. We divided slow-wave sleep% on day 1 by slow-wave sleep% on day 2 (slow-wave sleep%@day1 / slow-wave sleep%@day2) and multiplied the division by 100 for each experiment, and compared these values among experiments. In all experiments, the mean degree of slow-wave sleep% decrease was around 60% (Exp. 1: 64.3±11.06; Exp. 2: 56.3±10.49; Exp. 3: 63.0±7.67; mean ± SEM). There was no significant difference among experiments ($F_{2, 32}$=0.19, p=0.825, *n.s.*). This indicates that the degree of the FNE on the percentage of deep sleep was very similar among the experiments.

Table S2: Results of 4-way repeated measures ANOVA on SWA for Experiment 1, related to Figure 1

4-way ANOVA (factors=sleep stage, network, hemisphere, sleep session)				
4-way interaction	Network x Sleep stage x Hemisphere x Sleep session	$F_{3,30} = 4.45$	$p = 0.011$	*
3-way interactions	Network x Sleep stage x Hemisphere	$F_{3,30} = 1.82$	$p = 0.164$	
	Network x Sleep stage x Sleep session	$F_{3,30} = 2.50$	$p = 0.078$	
	Sleep stage x Hemisphere x Sleep session	$F_{1,10} = 0.41$	$p = 0.536$	
	Network x Hemisphere x Sleep session	$F_{3,30} = 2.21$	$p = 0.108$	
2-way interactions	Network x Sleep stage	$F_{3,30} = 37.63$	$p < 0.001$	****
	Network x Hemisphere	$F_{3,30} = 1.52$	$p = 0.229$	
	Network x Sleep session	$F_{3,30} = 4.00$	$p = 0.016$	*
	Sleep stage x Hemisphere	$F_{1,10} = 0.02$	$p = 0.879$	
	Sleep stage x Sleep session	$F_{1,10} = 9.59$	$p = 0.011$	*
	Hemisphere x Sleep session	$F_{1,10} = 0.71$	$p = 0.420$	
Main effects	Network	$F_{3,30} = 53.32$	$p < 0.001$	****
	Sleep stage	$F_{1,10} = 72.56$	$p < 0.001$	****
	Hemisphere	$F_{1,10} = 0.62$	$p = 0.450$	
	Sleep session	$F_{1,10} = 0.32$	$p = 0.587$	
3-way ANOVA for DMN (factors=sleep stage, hemisphere, sleep session)				
3-way interaction	Sleep stage x Hemisphere x Sleep session	$F_{1,10} = 7.39$	$p = 0.022$	*
2-way interactions	Sleep stage x Hemisphere	$F_{1,10} = 0.31$	$p = 0.592$	
	Sleep stage x Sleep session	$F_{1,10} = 18.07$	$p = 0.002$	***
	Hemisphere x Sleep session	$F_{1,10} = 8.02$	$p = 0.018$	*
Main effects	Sleep stage	$F_{1,10} = 64.64$	$p < 0.001$	****
	Hemisphere	$F_{1,10} = 1.47$	$p = 0.253$	
	Sleep session	$F_{1,10} = 0.66$	$p = 0.434$	
3-way ANOVA for ATN (factors=sleep stage, hemisphere, sleep session)				
3-way interaction	Sleep stage x Hemisphere x Sleep session	$F_{1,10} = 0.01$	$p = 0.926$	
2-way interactions	Sleep stage x Hemisphere	$F_{1,10} = 0.06$	$p = 0.807$	
	Sleep stage x Sleep session	$F_{1,10} = 3.24$	$p = 0.102$	
	Hemisphere x Sleep session	$F_{1,10} = 0.25$	$p = 0.626$	
Main effects	Sleep stage	$F_{1,10} = 75.90$	$p < 0.001$	****
	Hemisphere	$F_{1,10} = 0.80$	$p = 0.393$	
	Sleep session	$F_{1,10} = 0.24$	$p = 0.632$	
3-way ANOVA for SMN (factors=sleep stage, hemisphere, sleep session)				
3-way interaction	Sleep stage x Hemisphere x Sleep session	$F_{1,10} = 0.08$	$p = 0.781$	
2-way interactions	Sleep stage x Hemisphere	$F_{1,10} = 3.49$	$p = 0.091$	
	Sleep stage x Sleep session	$F_{1,10} = 12.90$	$p = 0.005$	**

	Hemisphere x Sleep session	$F_{1,10} = 0.06$	$p = 0.819$	
Main effects	Sleep stage	$F_{1,10} = 65.01$	$p < 0.001$	****
	Hemisphere	$F_{1,10} = 1.78$	$p = 0.212$	
	Sleep session	$F_{1,10} = 2.31$	$p = 0.159$	
3-way ANOVA for VIS (factors=sleep stage, hemisphere, sleep session)				
3-way interaction	Sleep stage x Hemisphere x Sleep session	$F_{1,10} = 0.03$	$p = 0.858$	
2-way interactions	Sleep stage x Hemisphere	$F_{1,10} = 1.74$	$p = 0.217$	
	Sleep stage x Sleep session	$F_{1,10} = 3.77$	$p = 0.081$	
	Hemisphere x Sleep session	$F_{1,10} = 1.89$	$p = 0.200$	
Main effects	Sleep stage	$F_{1,10} = 77.58$	$p < 0.001$	****
	Hemisphere	$F_{1,10} = 1.24$	$p = 0.291$	
	Sleep session	$F_{1,10} = 0.32$	$p = 0.584$	
2-way ANOVA for DMN during SWS (factors=hemisphere, sleep session)				
Interaction	Hemisphere x Sleep session	$F_{1,10} = 10.03$	$p = 0.010$	*
Main effects	Hemisphere	$F_{1,10} = 1.23$	$p = 0.294$	
	Sleep session	$F_{1,10} = 3.29$	$p = 0.100$	
2-way ANOVA for DMN during stage 2 sleep (factors=hemisphere, sleep session)				
Interaction	Hemisphere x Sleep session	$F_{1,10} = 2.55$	$p = 0.142$	
Main effects	Hemisphere	$F_{1,10} = 1.50$	$p = 0.249$	
	Sleep session	$F_{1,10} = 0.07$	$p = 0.794$	

****p<0.001, ***p<0.005, **p<0.01, *p<0.05.
Because interaction tests were critical, their results are shown in red.

Table S3: Subjective reports, related to Figures 3 and 4

		Day 1	Day 2	$Z_{(d.f.)}$	P
Subjective sleep-onset latency (min)	Exp. 2	16.2 ± 2.13	11.9 ± 1.33	$1.99_{(12)}$	0.046[a]
	Exp. 3	14.7 ± 2.81	10.8 ± 2.13	$2.04_{(10)}$	0.041[b]
Discomfort level	Exp. 2	1.7 ± 0.17	1.5 ± 0.14	$1.73_{(12)}$	0.083[c]
	Exp. 3	1.5 ± 0.16	1.2 ± 0.12	$1.34_{(10)}$	0.180[d]

See **2.2 Experimental design** in **Supplemental Experimental Procedures** for the measurement of subjective sleep-onset latency and discomfort level. Since data for Experiment 1 was not available, the table does not include Experiment 1.

Wilcoxon signed-rank test was applied to test whether subjective reports were significantly different between sleep sessions (day 1 vs. 2). The subjective sleep-onset latency was significantly longer on day 1 than day 2 for both experiments (**a** and **b**), while there was no significant difference in the discomfort level between days (**c** and **d**). This shows that the subjective discomfort level was not very high for day 1, which was not significantly different from day 2, irrespective of whether the FNE was clearly present or not.

SUPPLEMENTAL EXPERIMENTAL PROCEDURES

1. EXPERIMENT 1

1.1 Subjects

Eleven subjects (7 females; 23.6 ± 1.06 yrs, mean ± SEM) participated in Experiment 1. All subjects were right-handed. Subjects were screened to ensure the eligibility in the following way. After an experimenter thoroughly described the purpose and procedure of the experiment to candidates of subjects, they were asked to complete questionnaires regarding their sleep-wake habits; usual sleep and wake time, regularity of their sleep-wake habits and lifestyle, habits of nap-taking, and information regarding their physical and psychiatric health, including sleep complaints. Anyone who had a physical or psychiatric disease, was currently receiving medical treatment, or was suspected to have a sleep disorder was excluded. People who had the habit of consuming alcoholic beverages before sleep or smoking were also excluded. Only people who had regular sleep-wake cycles were included, i.e., differences between average bedtimes and sleep durations on weekdays and weekends were less than 2 hrs. The average sleep duration for each potential subject ranged from 6 to 9 hours regularly. All subjects gave written informed consent for their participation in experiments. The data collection was conducted at the Martinos center for Biomedical imaging, Massachusetts General Hospital. The research protocol was approved by the institutional review board.

1.2 Experimental design

Starting three days before the onset of the sleep session, subjects were instructed to maintain their regular sleep-wake habits, i.e., their daily wake/sleep time and sleep duration. On the day before the sleep session, they were instructed to refrain from alcohol consumption, unusual physical exercise, and nap taking. Their sleep-wake habits were monitored by a sleep log, and we confirmed that they maintained regular sleep-wake habits. Caffeine consumption was not allowed on the day of experiments.

MEG and PSG were measured during sleep in a supine position (see **1.3 MEG and PSG measurement**). The day 1 and day 2 sessions were conducted approximately a week apart so that any effects due to disrupted sleep during the first sleep session would not carry over to the second sleep session. Each subject's sleep time was set to approximate their habitual sleep time for both sessions, rather than enforcing a single uniform time. Room lights were turned off around midnight. The averaged habitual bedtime was 0:08 am. The averaged lights-off was 0:20 am on day 1, and 0:09 am on day 2. We conducted a one-way repeated measures ANOVA to test whether the lights-off time was significantly different among days (habitual bedtime, day 1, and day 2). However, no significant main effect of day was found ($F_{2,20}$=1.03, p=0.374). Thus, the lights-off time during experiments was not significantly different from the habitual lights-off time.

The total duration of recording time varied within the range of 90 to 180 min. We did not measure brain activity throughout the night, since it was difficult for subjects to sleep inside the MEG scanner without head motion for longer than 180 min in our experience [S15, S35]. The data analysis was limited to the first cycle of NREM sleep (stage 2 sleep and slow-wave sleep), since all subjects produced at least this length of data.

An MRI session was conducted separately after the completion of the sleep sessions (see **1.4 Anatomical and functional MRI acquisition**).

1.3 MEG and PSG measurement

MEG and PSG were simultaneously recorded in a magnetically shielded room (ELEKTA Neuromag, Helsinki, Finland).

MEG data were collected using the 306-channel whole-head Vectorview system (Elekta Neuromag, Helsinki, Finland) with 204 planar gradiometers and 102 magnetometers. PSG consisted of EEG,

electromyogram (EMG), electrooculogram (EOG), and electrocardiogram (ECG). EEG was recorded at 4 scalp sites (C3, C4, O1, O2) for 8 subjects and 7 scalp sites (C3, C4, O1, O2, Fz, Cz, Pz) for 3 subjects, according to the 10-20-electrode system referenced to the nasion. EOG was recorded from two electrodes placed at the outer canthi of both eyes (horizontal EOG). EMG was recorded bipolarly from the mentum. ECG was recorded with two electrodes placed at the right clavicle and the left rib bone. Electrode impedance was kept below 5 kΩ. Both MEG and EEG data were recorded at a sampling rate of 600 Hz. The data was filtered between 0.1 and 99 Hz, and was re-sampled at 200 Hz.

The positions of all scalp electrodes, anatomical landmarks including the nasion and two auricular landmarks, and four head-position indicator coils were measured using a FastTrack 3D digitizer (Polhemus, Colchester, VT). Head position within the MEG sensor array was measured at the beginning of the session. Five-minute empty room MEG recordings were also made immediately prior to each experiment for the purpose of estimating the noise covariance matrix [S9].

1.4 Anatomical and functional MRI acquisition

Anatomical MRI data were acquired and used for determining the conductor geometry for the boundary element model (BEM) of the head [S36], and for registering the MEG sensors' locations with the individual subject's anatomy [S1, S2]. Subjects were scanned in a 3T MR scanner (Trio, Siemens); a head coil was used in all experiments. Three T1-weighted MR images (MPRAGE; TR = 2.531 s, TE = 3.28 ms, flip angle = 7˚, TI = 1100 ms, 256 slices, voxel size = 1.3 x 1.3 x 1.0 mm) were acquired. The cortical surface was inflated for each participant for brain parcellation to localize individual gyri and sulci [S1, S2, S37, S38]. This information was used for the region-of-interest analysis for each network described later (see **Figure S1A** and **1.7 Brain networks** for definition of networks).

FMRI data were acquired to localize the early visual areas [S39, S40] using a gradient EPI sequence (TR = 2 s, TE = 30 ms, Flip Angle = 90º). Twenty-five contiguous slices (3 x 3 x 3.5 mm) orientated orthogonal to the calcarine sulcus were acquired covering the occipital to parieto-temporal cortices. Data were analyzed with FSFAST and FreeSurfer (http://surfer.nmr.mgh.harvard.edu) software. All functional images were motion corrected [S41], spatially smoothed with a Gaussian kernel of 5.0 mm (FWHM), and normalized individually across scans. Functional data were registered to the individual reconstructed brain [S1, S2].

1.5 Sleep-stage scoring

Sleep stages were scored for every 30-s epoch according to the standard criteria [S42] into: stage wakefulness (stage W), NREM stage 1 sleep (stage 1 sleep), NREM stage 2 sleep (stage 2 sleep), NREM stage 3 sleep + NREM stage 4 sleep (slow-wave sleep), and stage REM sleep. Since frontal EEG channels were not recorded in 8 out of 11 subjects, the amendment proposed by American Academy of Sleep Medicine [S7] was not applied to the scoring criteria. Sleep-onset was defined as the appearance of stage 2 sleep, in accordance with previous work [S15]. See **Table S1** for information on the sleep parameters.

1.6 Source localization of MEG in combination with MRI

To compute the strength of SWA, we used data from the first cycle of NREM sleep, because data were available for all the subjects (see **1.2 Experimental design**). MEG recordings were visually inspected to detect low quality channels, which constantly or periodically included artifacts or became flat, to be discarded from further analyses, since these would affect source localization. The number of excluded channels was only 4-5% for both days, 12.5 ± 2.15 for day1, and 16.3 ± 3.19 for day 2. They were not significantly different between days (Wilcoxon signed-rank test, z_{10}=1.52, p=0.130, *n.s.*). A Morlet wavelet analysis was applied to 306-channels MEG raw data [S8, S9] every 30s to obtain spectral power from 1-4 Hz, corresponding to the SWA frequency range [S43]. To localize the current sources underlying the MEG signals, we employed the cortically constrained minimum-norm estimate (MNE) using individual anatomical MRI and constrained the current locations to the cortical mantle [S8, S9]. Information from the MEG sensors' locations and the structural MRI segmentation were used to compute the forward solutions for all source locations using a three-layer model of boundary element method (BEM) [S36]. The individual forward solutions constituted the rows of the gain (lead-field) matrix. The noise covariance matrix was computed from the empty-room MEG data. These two matrices were used to calculate the

inverse operator to yield the estimated source activity, as a function of time, on a cortical surface [S8, S9]. We did not use EEG data for the source localization, because the number of EEG channels was too small (4-7 channels).

1.7 Brain networks

We selected well-established 4 brain networks: the DMN, ATN, SMN, and VIS. Here we first describe justification for selection of networks, and then their anatomical definitions.

SWA originates in cortical regions including such a brain network as the DMN [S44, S45]. Previous studies have shown that slow waves originate more frequently in prefrontal-orbitofrontal regions, which overlap with the DMN, and propagate in an anteroposterior direction [S46], and that sources of slow waves seem to overlap with the DMN [S47]. This is why we selected the DMN in the first place. In addition, we selected the other 3 networks such as ATN, SMN, and VIS, because it has been documented that these networks as well as the DMN are impacted by altered vigilance but still do not disappear during sleep [S46-S51]. Overall, these 4 networks made a good balance to examine SWA among networks in terms of the brain hierarchy: 2 higher associative networks (DMN and ATN) vs. 2 sensory and motor networks (SMN and VIS).

The locations of networks were anatomically determined *a priori* based on previously published papers, because the anatomical locations of the networks were extremely similar to those that have been reported in previous studies [S39, S40, S44, S45, S52-S61]. Anatomical locations of the regions of each network were identified through an automated parcellation method individually [S37, S38]. We defined the DMN as a circuit that includes the medial prefrontal, inferior parietal, and posterior parietal cortices, according to the previous research, which clarified the anatomical locations of the DMN [S44, S45]. The medial frontal cortex consists of the anterior part of superior frontal gyrus, and the anterior cingulate gyrus and sulcus. The inferior parietal cortex consists of the inferior parietal gyrus and angular gyrus. The posterior parietal cortex consists of the precuneus gyrus, posterior-dorsal cingulate gyrus, and sup-parietal sulcus.

The ATN was determined as a network, which consists of the frontal eye field (FEF), inferior and superior parietal cortices, the lateral frontal cortex, and temporoparietal junction, according to the previous study that clarified the anatomical locations of the ATN [S52]. FEF was defined as superior part of precentral sulcus and caudal part of superior frontal sulcus [S53]. Inferior and superior parietal cortices consisted of superior parietal gyrus and dorsal intraparietal sulcus [S53, S54]. Temporoparietal junction consisted of the inferior parietal gyrus supramarginal, temporal plane of the superior temporal gyrus, and posterior part of the middle temporal gyrus [S55]. The lateral frontal cortex consisted of middle frontal gyrus and opercular and triangular part of the inferior frontal gyrus [S54].

The SMN consisted of the primary motor area, somatosensory area, supplementary motor (SMA), and pre-supplementary (pre-SMA) areas [S56, S57], which we anatomically determined according to the brain parcellation method [S37, S38]. The primary motor and somatosensory areas are composed of the central sulcus, precentral gyrus, postcentral gyrus, and postcentral sulcus [S58]. The pre-SMA and the SMA were defined in accordance with previous studies [S59-S61]. First, three planes perpendicular to the AC-PC line; one through the rostral-most point of the genu of the corpus callosum (*vgcc*), one through the posterior margin of the anterior commissure (*vac*), and one through the posterior commissure (*vpc*) were defined. Next, the medial side of the superior frontal gyrus between *vgcc* and *vac* was defined as the pre-SMA, and a part of pre-central sulcus and the superior frontal gyrus between *vac* and *vpc* was defined as the SMA.

The VIS consisted of ventral and dorsal early visual areas (V1, V2, and V3) along the calcarine sulcus [S56, S57]. Additionally, we utilized a standard fMRI retinotopic mapping technique [S39, S40] for individually identifying these areas.

In the present study, we defined the networks based on anatomical information. Defining networks by anatomical landmarks may not necessarily be optimal and may present limitations in interpretation of results. However, the anatomical localization of the networks has been very consistent among previous established studies [S39, S40, S44, S45, S52-S61]. Thus, based on these previous studies, we have used the anatomical location information to define the networks in the present study.

1.8 Statistical analyses

The α level (Type I error rate) of 0.05 was set for all statistical analyses.

For repeated measures ANOVA, Mauchly's Test was conducted to test the assumption of sphericity. No sphericity violations were found in the present study. When a *n*-way (say, 4-way) repeated measures ANOVA showed a significant *n*-way (4-way) interaction, we conducted a (*n-1*)-way (3-way) repeated measures ANOVA using individual error terms rather than using pooled error terms, per each level of a factor [S62], to identify a simple interaction effect as a post-hoc analysis. We repeated this procedure until the source of interaction was finally identified at final *t*-tests. For instance, if we started off with a 4-way repeated measures ANOVA, which showed a significant 4-way interaction at the initial omnibus test, the final *t*-tests would correspond to simple-simple-simple effect tests. Because the initial omnibus ANOVA showed an *n*-way interaction, we were protected against inflating the Type 1 error rate in the following series of post-hoc analyses. This is a statistically well-established and valid way to avoid type 1 and type 2 errors [S62-S66].

When a *t*-test indicated a statistically significant difference, the effect size was calculated using Cohen's *d* [S67], which indicates the magnitude of the difference between two groups. It is interpreted as a large effect size when Cohen's $d \geq 0.8$, and as a medium effect size when $d \geq 0.5$.

Pearson's correlation was computed to test whether there was a significant correlation between the sleep-onset latency and SWA asymmetry index for each day. The correlation coefficients were compared between days by modified Pearson-Filon method [S68].

2. EXPERIMENT 2

2.1 Subjects

A new group of 13 subjects participated in experiment 2 (7 female; 25.2 ± 0.82 yrs, mean ± SEM). There were 11 right-handed and 2 left-handed subjects. See **1.1 Subjects** for the screening procedure. All subjects gave written informed consent for their participation in experiments. Data collection was conducted at Brown University. The research protocol was approved by the institutional review board.

2.2 Experimental design

Subjects were instructed to maintain their regular sleep-wake habits and to keep a sleep log for 3 days until the start of the experiment (see **1.2 Experimental design**). Subsequently, 2 experimental sleep sessions (day 1 and day 2) were conducted. The day 1 and day 2 sessions were conducted approximately a week apart so that any effects due to napping during the first sleep session would not carry over to the second sleep session. Caffeine consumption was not allowed on the day of experiments.

Subjects were informed that faint beep sounds might be presented through earphones while they were sleeping, but were instructed to ignore them. Room lights were turned off and the sleep session began, lasting for 90 min. PSG was monitored and sleep stages were scored in real time by experienced experimenters during the sleep session. Sound presentation (see **2.3 Auditory stimuli**) began after 5 min of an uninterrupted sleep stage [S7, S42], on either stage 2 sleep or slow-wave sleep. Sound presentations were stopped every time a lighter stage (stage W or stage 1) was observed. Sounds were not terminated during stage REM sleep. This procedure was repeated throughout the sleep session.

Immediately after completion of the sleep session, a questionnaire was administered to assess the subjective sleep quality including the subjective sleep-onset latency and the discomfort level. To measure the discomfort level, subjects were asked to give ratings on the scale of 1 to 4 (1. Very good, 2. Pretty good, 3. Not bad, 4. Not comfortable at all). See **Table S3** for the results.

In Experiment 2, sleep sessions began at approximately 2 pm. This time was chosen due to the known "mid-afternoon dip", which should facilitate the onset of sleep even in subjects who do not customarily nap [S69].

Data analyses were limited to the first cycle of NREM sleep, analogous to Experiment 1.

2.3 Auditory stimuli

Auditory stimuli were controlled by the MATLAB (The MathWorks, Inc.) software and presented through earphones (HAFR6A, JVC Americas Corp.). The stimuli consisted of 2000 Hz deviant (presented at 10% probability) and 1000 Hz standard (presented at 90% probability) pure tones, all 50 ms in duration (10 ms

rise/fall). These sounds were presented monaurally every 1s (1 trial = 1000 ms, fixed ISI = 950 ms). The probabilities of the sound types (deviant or standard) and the presented ear (left or right) were pseudo-randomized every 30 s, which corresponded to the sleep-stage scoring epoch (see **2.7 Sleep-stage scoring**), so that at least one deviant sound would be presented to each ear per epoch. More concretely, in a given 30-s epoch, 30 sounds would be presented in total, 15 per ear. Since the probability of a deviant sound was 10%, at least one deviant sound would be presented to each ear.

Sound intensity was approximately 32–35 dB (Extech 407740, Digital Sound Level Meter, Extech Instruments Corp.), which was lower than those used in previous studies (45–70 dB) [S22, S28] to prevent subjects from waking up. Before the sleep session began, it was confirmed that 35 dB was sufficiently quiet to maintain sleep, for each subject. However, with two participants who were awakened repeatedly by the 35 dB tones, intensity was lowered to 32 dB. Sound intensity was kept constant between the two sleep sessions.

It should be noted that there was no significant difference in the number of sound presentations between the hemispheres or sleep sessions. The total number of sound presentation was 666.5 ± 142.88 on day 1 and 784.2 ± 90.41 on day 2 (mean ± SEM) during slow-wave sleep. To test whether there was a significant difference in the number of sound presentation between the sleep sessions, we conducted a 3-way ANOVA (factors = sound type, hemisphere, sleep session) on the numbers of trials. The results indicated a significant main effect of sound type ($F_{1, 12}$=91.61, p<0.0001), as the biased frequency of the two sounds was the main manipulation (standard and deviant ratio = 90% and 10%). None of the other factors were significant (hemisphere, $F_{1, 12}$=1.67, p=0.221, *n.s.*; sleep session, $F_{1, 12}$=0.41, p=0.537, *n.s.*; sound type x hemisphere, $F_{1, 12}$=2.58, p=0.134, *n.s.*; sound type x sleep session, $F_{1, 12}$=0.39, p=0.545, *n.s.*; hemisphere x sleep session, $F_{1, 12}$=0.00, p=1.00, *n.s.*; sound type x hemisphere x sleep session, $F_{1, 12}$=0.17, p=0.689, *n.s.*). The results demonstrate that the number of sound presentations was not significantly different either between days or between the hemispheres. These results rule out the possibility that differences in brain responses can be accounted for by an inequality in the number of sound trials.

2.4 Analysis of brain responses to auditory stimuli

To test brain responses during sleep in association with the FNE, we examined an evoked brain potential known as the N3 [S25, S28, S70] from EEG data recorded during sleep using an oddball paradigm [S22, S28]. It has been shown that the amplitude of the N3 is one of negative ERP components that appear specifically during NREM sleep [S70] and increases in responses to rare and salient stimuli, especially during slow-wave sleep. The N3 has thus been used as an index of vigilance during deep sleep in humans [S25, S70]. The N3 is synonymous with the N550 component [S25, S28].

To obtain the N3, 4 frontal channels were analyzed (left: F5, F7; right: F6, F8). The N3 component has been reported to be dominantly observed in the frontal region, but to a much smaller degree in posterior region [S22, S25]. Thus, only frontal channels were chosen for the N3 ERP analysis. All data were examined visually for each trial, and any trials that included arousals (see **2.5 Scoring of arousals**) [S7, S71], motion artifacts, or eye movements in any of the 4 channels were excluded from further analyses. The numbers of excluded channels from the ERP analysis were very small; 0.2 ± 0.15 for day 1, and 0.1 ± 0.08 for day 2. They were not significantly different between days (Wilcoxon signed-rank test, z_{12}=0.45, p=0.655, *n.s.*).

The amplitudes of EEG during the 200 ms pre-stimulus period (-200 ms to 0 ms) were averaged. The mean amplitude EEG of the pre-stimulus period was subtracted from the EEG amplitudes from the 0 to 1000 ms post-stimulus period to normalize signal amplitude for each of 1-s trial (0 to 1000-ms post-stimulus). These normalized values were averaged for each sound type (deviant and standard), hemisphere (left and right), and sleep session (day 1 and day 2) during slow-wave sleep to compute averaged brain responses. Then the average value of the 650–955ms post-stimulus time window from the brain responses was used as the N3 amplitude for each condition. We chose this time window, since all the subjects showed the peak N3 amplitude during this period and it roughly corresponds to the previous studies [S24, S72].

2.5 Scoring of arousals

An arousal is defined as “an abrupt shift of EEG frequency including alpha, theta, and/or frequencies greater than 16 Hz (but not spindles) that lasts at least 3 seconds, with at least 10 seconds of a stable sleep

state preceding the change" [S7, S71]. Thus, an arousal is different from stage W, which is a scored sleep stage for a 30-sec epoch (see **2.7 Sleep-stage scoring**). Since an arousal has better temporal sensitivity than stage W, an arousal count was used in Experiment 2. Since hemispheric asymmetries in SWA and brain response were found only during slow-wave sleep, we scored the arousals that occurred specifically during this stage.

To investigate the number of arousals associated with deviant-sound presentations, we examined the hemisphere of presentation just before the arousal occurred in a 30-sec time window. First, we identified an arousal on EEG. Second, we detected the point of presentation of the deviant sound, which was the latest to the arousal. Third, we examined to which of the left and right ears the deviant sound was presented. If the last deviant sound was presented to the subjects' *right* ear immediately before the arousal occurrence, we classified this as a *left-hemisphere trial* (i.e. the contralateral hemisphere), and so on. This classification is based on a basic auditory-information processing theory [S73], according to which sounds presented to an ear are predominantly transferred to the contralateral hemisphere first, and the contralateral pathway blocks the ipsilateral pathway. Thus, we assume that sounds presented to the right ear are primarily projected to the left hemisphere. Likewise, the sounds presented to the left ear will be projected to the right hemisphere.

2.6 PSG measurement

PSG was recorded in a soundproof and shielded room. PSG consisted of EEG, EOG, EMG, and ECG. EEG was recorded at 64 scalp sites according to the 10% electrode position [S74] using active electrodes (actiCap, Brain Products, LLC) with a standard amplifier (BrainAmp Standard, Brain Products, LLC). The online reference was Fz, and it was re-referenced to the average of the left and right mastoids offline after the recording. Sampling frequency was 500 Hz. The impedance was kept below 20 kΩ (the active electrodes included a new type of integrated impedance converter, which allowed them to transmit the EEG signal with significantly lower levels of noise than traditional passive electrode systems). The data quality with active electrodes was as good as 5 kΩ using passive electrodes, which were used for EOG, EMG, and ECG (BrainAmp ExG, Brain Products, LLC). Horizontal EOG was recorded from 2 electrodes placed at the outer canthi of both eyes. Vertical EOG was measured from 4 electrodes 3 cm above and below both eyes. EMG was recorded from the mentum (chin). ECG was recorded from 2 electrodes placed at the right clavicle and the left rib bone. The impedance was kept below 10 kΩ for the passive electrodes. Brain Vision Recorder software (Brain Products, LLC) was used for recording. The data was filtered between 0.1 and 40 Hz.

2.7 Sleep-stage scoring

Sleep stages were scored for every 30-s epoch, following standard criteria [S7, S42], into stage wakefulness (stage W), NREM stage 1 sleep (stage 1 sleep), NREM stage 2 sleep (stage 2 sleep), NREM stage 3 sleep (slow-wave sleep), and stage REM sleep. The amendment by American Academy of Sleep Medicine [S7] was applied to the criteria for Experiment 2. See **Table S1** for information on the sleep parameters.

2.8 Statistical analyses

The α level (Type I error rate) of 0.05 was set for all statistical analyses. The same procedures described in **1.8 Statistical analyses** were used for repeated measures ANOVA. The nonparametric Wilcoxon signed-rank test was applied to the total number of arousals per min during slow-wave sleep and the arousal occurrence (%), since the normal distribution of these data was not assumed. The false discovery rate (FDR) was controlled to be at 0.05 for multiple comparisons [S75] for Wilcoxon signed-rank tests (**Figure 3B**).

3. EXPERIMENT 3

3.1 Subjects

Another new group of 11 subjects participated in Experiment 3 (9 female; 24.0 ± 0.77 yrs, mean ± SEM). See **1.1 Subjects** for the screening procedure. There were 1 left-handed and 10 right-handed subjects. All

subjects gave written informed consent for their participation in experiments. Data collection was conducted at Brown University. The research protocol was approved by the institutional review board.

3.2 Experimental design

Subjects were instructed to maintain their regular sleep-wake habits and to keep a sleep log for 3 days until the start of the experiment (see **1.2 Experimental design**). Subsequently, 2 experimental sleep sessions (day 1 and day 2) were conducted. The day 1 and day 2 sessions were conducted approximately a week apart so that any effects due to napping during the first sleep session would not carry over to the second sleep session. Caffeine consumption was not allowed on the day of the experiments.

Subjects were informed that faint beep sounds might be presented through earphones while they were sleeping. They were asked to tap their fingers at least 3 times using their index finger and thumb of the non-dominant hand if they heard any sounds. They were also instructed not to be intensively alert to catch the sound to make responses. This instruction was given to prevent the subjects from showing extreme poor sleep due to their heightened motivation to perfect behavioral responses. Room lights were turned off and the sleep session began, around at 2 pm, and lasted 90 min, analogously to Experiment 2 (see **2.2 Experimental design**) [S69]. Experienced experimenters monitored the PSG recording, and scored sleep stages in real time during the sleep session. The start of sound presentation (see **2.3 Auditory stimuli**) was aimed at around the onset of slow-wave sleep. To do so online, we set the criteria according to which sound presentation should start after at least 5 min of uninterrupted sleep from the lights-off and 3 clear slow waves at a frontal recording (Fz) appeared. Sound presentations were stopped when a signature of stage W (see **2.7 Sleep-stage scoring**) was observed and a tapping response was made (see **3.5 PSG and finger motion measurements**). After the awakening, sound presentations were resumed only when the above-mentioned criteria (stable sleep and 3 slow waves at Fz) were met. However, most subjects did not meet the criteria for the second time within 90 min. Thus, further analyses on behavioral data were limited to the time interval between lights-off and the first awakening and behavioral response, for all the subjects showed at least one awakening and behavioral response.

Immediately after completion of the sleep session, a questionnaire was administered to assess subjective sleep quality including the subjective sleep-onset latency and discomfort level (see **2.2 Experimental design**). See **Table S3** for the results.

3.3 Auditory stimuli

Auditory stimuli were controlled by the MATLAB (The MathWorks, Inc.) software and presented through earphones (HAFR6A, JVC Americas Corp.). The parameters for sounds, including the frequency, probability, and duration for auditory stimuli, were identical to those of Experiment 2 (see **2.3 Auditory stimuli**, **2.7 Sleep-stage scoring**), except the manipulation of the sound intensity (Extech 407740, Digital Sound Level Meter, Extech Instruments Corp.). Since Experiment 3 was aimed at measuring how fast the tapping would be made upon awakening from slow-wave sleep, the sound intensity was controlled to be closely around the awakening threshold [S76], and not to exceed the threshold. The initial sound intensity was set to 30 dB, which was considered to be lower than the awakening thresholds for most people [S76]. The sound intensity was increased gradually until it reached the awakening threshold over which subjects were woken and made a tapping response (see **3.2 Experimental design**). If a subject continued to sleep and did not make a tapping response for a certain time period with a given intensity, this suggested that the intensity was significantly lower than the awakening threshold [S76]. In such a case, the sound intensity was increased by 2 dB deliberately. Since the awakening threshold is varied with sleep depth [S76-S78], the intensity was increased every 3 min if slow waves were sporadic in a 30-s epoch (likely to be in stage 2 sleep) and every 1 min if slow waves were abundantly seen in a 30-s epoch (likely to be in slow-wave sleep).

Although the intensity of the sounds used was exactly the same between hemispheres on both days, the subjects were woken by a slightly but significantly weaker sound on day 1 than day 2 in general (mean ± SEM, day 1: 38.0 ± 2.24 dB, day 2: 41.8 ± 2.80 dB, Wilcoxon signed-rank test, $z(10)=2.06$, $p=0.040$). The awakening threshold on day 2 was comparable to a previous study that was without the FNE [S76].

It should be noted that the hemispheric asymmetry in the reaction time on day 1 (shown in **Figure 4, Figure S4A & S4B**) is not due to differences in the properties of the sounds presented. First, the intensity

of the sounds was *weaker*, not stronger, on day 1 than on day 2. Second, the other parameters for sounds, including the frequency, probability, and duration were exactly the same between hemispheres and days (see **2.3 Auditory stimuli**). See **Figure S4** for additional information on the reaction times.

3.4 Behavioral responses to auditory stimuli

Tapping responses were detected in EMG attached to fingers (see **3.5 PSG and finger motion measurements** below). If 3 or more conspicuous successive negative peaks occurred during wakefulness on EMG, we regarded this as a tapping response. The reaction time here was defined as the time interval between the start of the deviant sound presentation and the first tapping response.

We sorted left- and right-hemisphere trials based on which hemisphere the last deviant sound was presented to before awakening occurred, in a similar way to Experiment 2 [S73] (see **2.5 Scoring of arousals**).

3.5 PSG and finger motion measurements

PSG was recorded in a soundproof and shielded room. PSG consisted of EEG, EOG, and EMG. EEG was recorded at 23 scalp sites according to the 10% electrode position [S74] using active electrodes (actiCap, Brain Products, LLC) with a standard amplifier (BrainAmp Standard, Brain Products, LLC). The online reference was Cz, and it was re-referenced to the average of the left and right mastoids offline after the recording. Sampling frequency was 500 Hz. The impedance was kept below 20 kΩ (see 2.6 for the data quality of active electrodes). Horizontal EOG was recorded from 2 electrodes placed at the outer canthi of both eyes. Vertical EOG was measured from 4 electrodes 3 cm above and below both eyes. EMG for PSG was recorded from the mentum (chin). Finger tapping was detected by EMG measured from the bipolar electrodes attached to metacarpophalangeal joint of the index finger and thumb carpometacarpal [S79] of the non-dominant hand. The impedance was kept below 10 kΩ for EOG and EMG, and 30 kΩ for finger tap motion. The impedance for finger motion was set to a higher value compared to EOG or chin EMG, since this value was sufficient to measure conspicuous finger tap motions. Brain Vision Recorder software (Brain Products, LLC) was used for recording. The data was filtered between 0.1 and 40 Hz.

3.6 Sleep-stage scoring

The same procedures as described in **2.7 Sleep-stage scoring** were used.

3.7 Spectral power and correlation analyses

To obtain regional SWA (1–4 Hz) during slow-wave sleep, a fast-Fourier transformation was applied to EEG data in 5-second epochs and smoothed with a tapered cosine window [S80]. Six epochs were averaged to yield the averaged spectral data of 30 s. The SWA strength per 30 s was averaged across 6 channels for each hemisphere. The six channels were chosen from anterior and posterior regions (left hemisphere: F3, F5, F7, P3, P5, P7; right hemisphere: F4, F6, F8, P4, P6, P8) near the medial frontal [S11] and parietal cortices [S12] in possible coverage of the DMN. The obtained SWA were then compared between hemispheres and sleep sessions.

We next obtained an SWA asymmetry index by [left SWA - right SWA]/[left SWA + right SWA] for each of sleep sessions. Pearson's correlation was then computed between the time interval from a deviant sound to awakening and to tapping (see **3.4 Behavioral responses to auditory stimuli** and **Figure S4B**) and the SWA asymmetry index for each sleep session.

3.8 Statistical analyses

The alpha level (type I error rate) of 0.05 was set for all statistical analyses. Non-parametric tests were conducted on the number of subjects and the reaction time data, which do not follow normal distribution [S81]. The McNemar's test was conducted on the number of subjects who were woken on a left-hemisphere or right-hemisphere trial on day 1 and day 2 to test whether the numbers of subjects who were woken on a left-hemisphere trial were different between the days (**Figure 4A**). The reaction time data was first log-transformed to reduce the skew of data [S81]. Then, the Mann-Whitney U test was conducted on

the log-transformed reaction time data (**Figure 4B**, **Figure S4**). The FDR was controlled to be at 0.05 for multiple comparisons [S75] for reaction time data shown in **Figure S4**.

4. Comparison of sleep parameters among Experiments 1-3

To confirm that the FNE occurred in all three experiments (Exp.1–3) to comparable amounts, we compared 3 important sleep parameters (shown in **Table S1**) to measure the FNE [S29-S31] among these experiments. The 3 parameters were the sleep-onset latency (see **1.5 Sleep-stage scoring**), wake after sleep onset (WASO, the time spent in stage W in min after sleep onset), and the percentage of slow-wave sleep (slow-wave sleep%) within the first sleep cycle.

For a statistical comparison, a 2-way mixed-design ANOVA (factors = experiment and sleep session) was conducted on each of the 3 sleep parameters measured in 3 different experiments (Exp. 1-3). Note that a different set of subjects participated in each experiment. Thus, a mixed design ANOVA was used since the factor of experiment (Exp. 1 vs. 2 vs. 3) was a between-subjects variable, and the factor of sleep session (day 1 vs. day 2) was a within-subjects variable. As a post-hoc test, a two-tailed paired *t*-test was conducted for within-subjects comparisons (day 1 vs. day 2), since this comparison would clarify the presence of the FNE. The effect size was calculated using Cohen's *d* (see **1.8 Statistical analyses**). For the analysis of slow-wave sleep%, the Scheffé's method was taken for between-subjects comparisons where there were 3 levels (Exp. 1 vs. 2 vs. 3) to control for the Type I error rate. See **Table S1** for the detailed results.

Additionally, other standard sleep variables within the first sleep cycle and total recording time are shown in **Table S1**, to indicate a general sleep structure for each experiment. Sleep variables include the percentage of each sleep stage, sleep efficiency (SE, the total percentage spent in stage 1, 2, and slow-wave sleep), and the total sleep time. To calculate the percentage of each sleep stage, we divided the time spent in each sleep stage by the total time of the first sleep cycle. Data in **Table S1** did not include stage REM sleep, except the total recording time (see **1.2 Experimental design**).

Supplemental References

S1. Fischl, B., Sereno, M.I., and Dale, A.M. (1999). Cortical surface-based analysis. II: Inflation, flattening, and a surface-based coordinate system. Neuroimage *9*, 195-207.

S2. Dale, A.M., Fischl, B., and Sereno, M.I. (1999). Cortical surface-based analysis. I. Segmentation and surface reconstruction. Neuroimage *9*, 179-194.

S3. Amzica, F., and Steriade, M. (1997). The K-complex: its slow (<1-Hz) rhythmicity and relation to delta waves. Neurology *49*, 952-959.

S4. Jahnke, K., von Wegner, F., Morzelewski, A., Borisov, S., Maischein, M., Steinmetz, H., and Laufs, H. (2012). To wake or not to wake? The two-sided nature of the human K-complex. Neuroimage *59*, 1631-1638.

S5. Laurino, M., Menicucci, D., Piarulli, A., Mastorci, F., Bedini, R., Allegrini, P., and Gemignani, A. (2014). Disentangling different functional roles of evoked K-complex components: Mapping the sleeping brain while quenching sensory processing. Neuroimage *86*, 433-445.

S6. Colrain, I.M., Webster, K.E., and Hirst, G. (1999). The N550 component of the evoked K-complex: a modality non-specific response? J. Sleep Res. *8*, 273-280.

S7. Iber, C., Ancoli-Israel, S.S., Chesson, A., and Quan, S.F. (2007). The AASM Manual for the Scoring of Sleep and Associated Events: Rules, Terminology, and Technical Specifications (Westchester: American Academy of Sleep Medicine).

S8. Lin, F.H., Witzel, T., Hamalainen, M.S., Dale, A.M., Belliveau, J.W., and Stufflebeam, S.M. (2004). Spectral spatiotemporal imaging of cortical oscillations and interactions in the human brain. Neuroimage *23*, 582-595.

S9. Ahveninen, J., Lin, F.H., Kivisaari, R., Autti, T., Hamalainen, M., Stufflebeam, S., Belliveau, J.W., and Kahkonen, S. (2007). MRI-constrained spectral imaging of benzodiazepine modulation of spontaneous neuromagnetic activity in human cortex. Neuroimage *35*, 577-582.

S10. Czisch, M., Wetter, T.C., Kaufmann, C., Pollmacher, T., Holsboer, F., and Auer, D.P. (2002). Altered processing of acoustic stimuli during sleep: reduced auditory activation and visual deactivation detected by a combined fMRI/EEG study. Neuroimage *16*, 251-258.

S11. Gehring, W.J., and Willoughby, A.R. (2002). The medial frontal cortex and the rapid processing of monetary gains and losses. Science *295*, 2279-2282.

S12. Arzy, S., Thut, G., Mohr, C., Michel, C.M., and Blanke, O. (2006). Neural basis of embodiment: distinct contributions of temporoparietal junction and extrastriate body area. J. Neurosci. *26*, 8074-8081.

S13. Sel, A., Forster, B., and Calvo-Merino, B. (2014). The emotional homunculus: ERP evidence for independent somatosensory responses during facial emotional processing. J. Neurosci. *34*, 3263-3267.

S14. Cravo, A.M., Rohenkohl, G., Wyart, V., and Nobre, A.C. (2013). Temporal expectation enhances contrast sensitivity by phase entrainment of low-frequency oscillations in visual cortex. J. Neurosci. *33*, 4002-4010.

S15. Tamaki, M., Huang, T.R., Yotsumoto, Y., Hamalainen, M., Lin, F.H., Nanez, J.E., Sr., Watanabe, T., and Sasaki, Y. (2013). Enhanced spontaneous oscillations in the supplementary motor area are associated with sleep-dependent offline learning of finger-tapping motor-sequence task. J. Neurosci. *33*, 13894-13902.

S16. Weitzman, E.D., and Kremen, H. (1965). Auditory evoked responses during different stages of sleep in man. Electroencephalogr. Clin. Neurophysiol. *18*, 65-70.

S17. Ujszaszi, J., and Halasz, P. (1986). Late component variants of single auditory evoked responses during NREM sleep stage 2 in man. Electroencephalogr. Clin. Neurophysiol. *64*, 260-268.

S18. Ujszaszi, J., and Halasz, P. (1988). Long latency evoked potential components in human slow wave sleep. Electroencephalogr. Clin. Neurophysiol. *69*, 516-522.

S19. Colrain, I.M. (2005). The K-complex: a 7-decade history. Sleep *28*, 255-273.

S20. Sallinen, M., Kaartinen, J., and Lyytinen, H. (1994). Is the appearance of mismatch negativity during stage 2 sleep related to the elicitation of K-complex? Electroencephalogr. Clin. Neurophysiol. *91*, 140-148.
S21. Paavilainen, P., Alho, K., Reinikainen, K., Sams, M., and Naatanen, R. (1991). Right hemisphere dominance of different mismatch negativities. Electroencephalogr. Clin. Neurophysiol. *78*, 466-479.
S22. Nielsen-Bohlman, L., Knight, R.T., Woods, D.L., and Woodward, K. (1991). Differential auditory processing continues during sleep. Electroencephalogr. Clin. Neurophysiol. *79*, 281-290.
S23. Sutton, S., Braren, M., Zubin, J., and John, E.R. (1965). Evoked-potential correlates of stimulus uncertainty. Science *150*, 1187-1188.
S24. Bastuji, H., Garcia-Larrea, L., Franc, C., and Mauguiere, F. (1995). Brain processing of stimulus deviance during slow-wave and paradoxical sleep: a study of human auditory evoked responses using the oddball paradigm. J. Clin. Neurophysiol. *12*, 155-167.
S25. Bastuji, H., and Garcia-Larrea, L. (1999). Evoked potentials as a tool for the investigation of human sleep. Sleep Med. Rev. *3*, 23-45.
S26. Picton, T.W., and Hillyard, S.A. (1974). Human auditory evoked potentials. II. Effects of attention. Electroencephalogr. Clin. Neurophysiol. *36*, 191-199.
S27. Hillyard, S.A., Hink, R.F., Schwent, V.L., and Picton, T.W. (1973). Electrical signs of selective attention in the human brain. Science *182*, 177-180.
S28. Michida, N., Hayashi, M., and Hori, T. (2005). Effects of hypnagogic imagery on the event-related potential to external tone stimuli. Sleep *28*, 813-818.
S29. Webb, W.B., and Campbell, S.S. (1979). The first night effect revisited with age as a variable. Waking Sleeping *3*, 319-324.
S30. Schmidt, H.S., and Kaelbling, R. (1971). The differential laboratory adaptation of sleep parameters. Biol. Psychiatry *3*, 33-45.
S31. Tamaki, M., Nittono, H., Hayashi, M., and Hori, T. (2005). Examination of the first-night effect during the sleep-onset period. Sleep *28*, 195-202.
S32. Nofzinger, E.A., Nissen, C., Germain, A., Moul, D., Hall, M., Price, J.C., Miewald, J.M., and Buysse, D.J. (2006). Regional cerebral metabolic correlates of WASO during NREM sleep in insomnia. J. Clin. Sleep Med. *2*, 316-322.
S33. Kales, A., Jacobson, A., Kales, J.D., Kun, T., and Weissbuch, R. (1967). All-night EEG sleep measurements in young adults. Psychonom. Sci. *7*, 67-68.
S34. Scharf, M.B., Kales, A., and Bixler, E.O. (1975). Readaptation to the sleep laboratory in insomniac subjects. Psychophysiology *12*, 412-415.
S35. Bang, J.W., Khalilzadeh, O., Hamalainen, M., Watanabe, T., and Sasaki, Y. (2014). Location specific sleep spindle activity in the early visual areas and perceptual learning. Vision Res. *99*, 162-171.
S36. Hamalainen, M.S., and Sarvas, J. (1989). Realistic conductivity geometry model of the human head for interpretation of neuromagnetic data. IEEE Trans. Biomed. Eng. *36*, 165-171.
S37. Fischl, B., van der Kouwe, A., Destrieux, C., Halgren, E., Segonne, F., Salat, D.H., Busa, E., Seidman, L.J., Goldstein, J., Kennedy, D., et al. (2004). Automatically parcellating the human cerebral cortex. Cereb. Cortex *14*, 11-22.
S38. Destrieux, C., Fischl, B., Dale, A., and Halgren, E. (2010). Automatic parcellation of human cortical gyri and sulci using standard anatomical nomenclature. Neuroimage *53*, 1-15.
S39. Engel, S.A., Rumelhart, D.E., Wandell, B.A., Lee, A.T., Glover, G.H., Chichilnisky, E.J., and Shadlen, M.N. (1994). fMRI of human visual cortex. Nature *369*, 525.
S40. Yotsumoto, Y., Watanabe, T., and Sasaki, Y. (2008). Different dynamics of performance and brain activation in the time course of perceptual learning. Neuron *57*, 827-833.
S41. Cox, R.W., and Jesmanowicz, A. (1999). Real-time 3D image registration for functional MRI. Magn. Reson. Med. *42*, 1014-1018.
S42. Rechtschaffen, A., and Kales, A. (1968). A Manual of Standardized Terminology, Techniques, and Scoring System for Sleep Stages of Human Subjects (Washington, DC: Public Health Service, US Government Printing Office).

S43. Huber, R., Ghilardi, M.F., Massimini, M., and Tononi, G. (2004). Local sleep and learning. Nature *430*, 78-81.
S44. Mason, M.F., Norton, M.I., Van Horn, J.D., Wegner, D.M., Grafton, S.T., and Macrae, C.N. (2007). Wandering minds: the default network and stimulus-independent thought. Science *315*, 393-395.
S45. Raichle, M.E., MacLeod, A.M., Snyder, A.Z., Powers, W.J., Gusnard, D.A., and Shulman, G.L. (2001). A default mode of brain function. Proc. Natl. Acad. Sci. USA *98*, 676-682.
S46. Massimini, M., Huber, R., Ferrarelli, F., Hill, S., and Tononi, G. (2004). The sleep slow oscillation as a traveling wave. J. Neurosci. *24*, 6862-6870.
S47. Murphy, M., Riedner, B.A., Huber, R., Massimini, M., Ferrarelli, F., and Tononi, G. (2009). Source modeling sleep slow waves. Proc. Natl. Acad. Sci. USA *106*, 1608-1613.
S48. Horovitz, S.G., Fukunaga, M., de Zwart, J.A., van Gelderen, P., Fulton, S.C., Balkin, T.J., and Duyn, J.H. (2008). Low frequency BOLD fluctuations during resting wakefulness and light sleep: a simultaneous EEG-fMRI study. Hum. Brain Mapp. *29*, 671-682.
S49. Larson-Prior, L.J., Zempel, J.M., Nolan, T.S., Prior, F.W., Snyder, A.Z., and Raichle, M.E. (2009). Cortical network functional connectivity in the descent to sleep. Proc. Natl. Acad. Sci. USA *106*, 4489-4494.
S50. Buysse, D.J., Germain, A., Hall, M., Monk, T.H., and Nofzinger, E.A. (2011). A Neurobiological model of insomnia. Drug Discov. Today Dis. Models *8*, 129-137.
S51. Dang-Vu, T.T., Schabus, M., Desseilles, M., Albouy, G., Boly, M., Darsaud, A., Gais, S., Rauchs, G., Sterpenich, V., Vandewalle, G., et al. (2008). Spontaneous neural activity during human slow wave sleep. Proc. Natl. Acad. Sci. USA *105*, 15160-15165.
S52. Corbetta, M., and Shulman, G.L. (2002). Control of goal-directed and stimulus-driven attention in the brain. Nat. Rev. Neurosci. *3*, 201-215.
S53. Kastner, S., Pinsk, M.A., De Weerd, P., Desimone, R., and Ungerleider, L.G. (1999). Increased activity in human visual cortex during directed attention in the absence of visual stimulation. Neuron *22*, 751-761.
S54. Shulman, G.L., d'Avossa, G., Tansy, A.P., and Corbetta, M. (2002). Two attentional processes in the parietal lobe. Cereb. Cortex *12*, 1124-1131.
S55. Downar, J., Crawley, A.P., Mikulis, D.J., and Davis, K.D. (2000). A multimodal cortical network for the detection of changes in the sensory environment. Nat. Neurosci. *3*, 277-283.
S56. Yeo, B.T., Krienen, F.M., Sepulcre, J., Sabuncu, M.R., Lashkari, D., Hollinshead, M., Roffman, J.L., Smoller, J.W., Zollei, L., Polimeni, J.R., et al. (2011). The organization of the human cerebral cortex estimated by intrinsic functional connectivity. J. Neurophysiol. *106*, 1125-1165.
S57. Buckner, R.L., Krienen, F.M., and Yeo, B.T. (2013). Opportunities and limitations of intrinsic functional connectivity MRI. Nat. Neurosci. *16*, 832-837.
S58. Grafton, S.T., Woods, R.P., Mazziotta, J.C., and Phelps, M.E. (1991). Somatotopic mapping of the primary motor cortex in humans: activation studies with cerebral blood flow and positron emission tomography. J. Neurophysiol. *66*, 735-743.
S59. Crosson, B., Sadek, J.R., Bobholz, J.A., Gokcay, D., Mohr, C.M., Leonard, C.M., Maron, L., Auerbach, E.J., Browd, S.R., Freeman, A.J., et al. (1999). Activity in the paracingulate and cingulate sulci during word generation: an fMRI study of functional anatomy. Cereb. Cortex *9*, 307-316.
S60. Hikosaka, O., Sakai, K., Miyauchi, S., Takino, R., Sasaki, Y., and Putz, B. (1996). Activation of human presupplementary motor area in learning of sequential procedures: a functional MRI study. J. Neurophysiol. *76*, 617-621.
S61. Picard, N., and Strick, P.L. (2001). Imaging the premotor areas. Curr. Opin. Neurobiol. *11*, 663-672.
S62. Keselman, H.J., and Keselman, J.C. (1993). Analysis of repeated measurements. In Applied Analysis of Variance in Behavioral Science, L.K. Edwards, ed. (New York: Marcel Dekker), pp. 105-145.
S63. Cohen, B.H. (2004). Explaining Psychological Statistics (New York: John Wiley & Sons).

S64. Rosnow, R.L., and Rosenthal, R. (1995). “Some things you learn aren’t so”: Cohen’s paradox, Asch’s paradigm, and the interpretation of interaction. Psychol. Sci. *6*, 3-9.
S65. Lubin, A. (1961). The interpretation of significant interaction. J. Educ. Psychol. Meas. *21*, 807-817.
S66. Garson, G.D. (2012). General Linear Models: Univariate GLM, Anova/Ancova, Repeated Measures (Statistical Associates Blue Book Series 19) [Kindle Edition] (Statistical Associates Publishers).
S67. Cohen, J. (1988). Statistical Power Analysis for the Behavioral Sciences (Hillsdale: Lawrence Erlbaum and Associates).
S68. Raghunathan, T.E., Rosenthal, R., and Rubin, D.B. (1996). Comparing correlated but nonoverlapping correlations. Psychol. Methods *1*, 178-183.
S69. Horikawa, T., Tamaki, M., Miyawaki, Y., and Kamitani, Y. (2013). Neural decoding of visual imagery during sleep. Science *340*, 639-642.
S70. Atienza, M., Cantero, J.L., and Escera, C. (2001). Auditory information processing during human sleep as revealed by event-related brain potentials. Clin. Neurophysiol. *112*, 2031-2045.
S71. Bonnet, M., Carley, D., Carskadon, M., Easton, P., Guilleminault, C., Harper, R., Hayes, B., Hirshkowitz, M., Ktonas, P., Keenan, S., Pressman, M., Roehrs, T., Smith, J., Walsh, J., Weber, S., Westbrook, P., Jordan, B. (1992). EEG arousals: scoring rules and examples: a preliminary report from the Sleep Disorders Atlas Task Force of the American Sleep Disorders Association. Sleep *15*, 173-184.
S72. Perrin, F., Garcia-Larrea, L., Mauguiere, F., and Bastuji, H. (1999). A differential brain response to the subject's own name persists during sleep. Clin. Neurophysiol. *110*, 2153-2164.
S73. Kimura, D. (1967). Functional asymmetry of the brain in dichotic listening. Cortex *3*, 163-178.
S74. Sharbrough, F.C.G.E., Lesser, R.P., Lüders, H., Nuwer, M., and Picton, T.W. (1991). American electroencephalographic society guidelines for standard electrode position nomenclature. J. Clin. Neurophysiol. *8*, 200-202.
S75. Benjamini, Y., and Y., H. (1995). Controlling the false discovery rate: A practical and powerful approach to multiple testing. J. R. Stat. Soc. Ser. B Stat. Methodol. *57*, 289-300.
S76. Goodenough, D.R., Lewis, H.B., Shapiro, A., Jaret, L., and Sleser, I. (1965). Dream reporting following abrupt and gradual awakenings from different types of sleep. J. Pers. Soc. Psychol. *2*, 170-179.
S77. Williams, H.L., Hammack, J.T., Daly, R.L., Dement, W.C., and Lubin, A. (1964). Responses to auditory stimulation, sleep loss and the EEG stages of sleep. Electroencephalogr. Clin. Neurophysiol. *16*, 269-279.
S78. Rechtschaffen, A., Hauri, P., and Zeitlin, M. (1966). Auditory awakening thresholds in REM and NREM sleep stages. Percept. Mot. Skills *22*, 927-942.
S79. Arunachalam, R., Weerasinghe, V.S., and Mills, K.R. (2005). Motor control of rapid sequential finger tapping in humans. J. Neurophysiol. *94*, 2162-2170.
S80. Nobili, L., Baglietto, M.G., De Carli, F., Savoini, M., Schiavi, G., Zanotto, E., Ferrillo, F., and De Negri, M. (1999). A quantified analysis of sleep electroencephalography in anorectic adolescents. Biol Psychiatry *45*, 771-775.
S81. Luce, R.D. (1986). Response time distributions in memory search: a caution. In Human Memory and Cognitive Capabilities, F. Klix and H. Hagendorf, eds. (North-Holland: Elsevier Science Publishers B.V), pp. 109-121.